1-1-2020

Chronostratigraphy, site formation, and palaeoenvironmental context of late pleistocene and holocene occupations at grassridge rock shelter (Eastern Cape, South Africa)

Christopher J.H. Ames
University of Wollongong, cames@uow.edu.au

Luke A. Gliganic
lukeg@uow.edu.au

Carlos Cordova

Kelsey Boyd
University of Wollongong

Brian G. Jones
University of Wollongong, briangj@uow.edu.au

See next page for additional authors

Chronostratigraphy, site formation, and palaeoenvironmental context of late pleistocene and holocene occupations at grassridge rock shelter (Eastern Cape, South Africa)

Abstract

© 2020 The Author(s). Grassridge rock shelter is located in the high elevation grassland foothills of the Stormberg Mountains in the Eastern Cape of South Africa. This places Grassridge at an important biogeoclimatic intersec-tion between the Drakensberg Mountains, the South African coastal zone, and the interior arid lands of southern Africa. First excavated in 1979, the approximately 1.5 m stratigraphic sequence was divided into two major occupational components: a 50–70 cm thick Later Stone Age component dating between 7–6 ka and an underlying 50–80 cm thick Middle Stone Age component dated to 36 ka at the base. Here we present a reanalysis of the Grassridge stratigraphic sequence that combines new optically stimulated luminescence and radiocarbon age estimates with sedimentological and microbotanical analyses to evalu-ate site formation processes and the palaeoenvironmental context of human occupations. Results indicate a complex history of geogenic, anthropogenic, and biogenic inputs to the depositional sequence that are interspersed with pulsed human occupation from 43–28 ka, 13.5–11.6 ka, and 7.3–6.8 ka. Microbotanical remains indicate a cooler, drier grassland environment in MIS 3 that transitions to a warmer, moister grassland environment dominated by summer rainfall in the middle of MIS 1. The pulsed occupational sequence identified at Grassridge is characteristic of the Pleistocene and Holocene record across the greater high elevation grassland region of South Africa, which, based on comparison with other currently available evidence, seems linked to a complex system of forager mobility entwined with rapidly fluctuating palaeoenvironments across the last glacial to interglacial transition.

Publication Details

Ames, C. J.H., Gliganic, L., Cordova, C. E., Boyd, K., Jones, B. G., Maher, L. & Collins, B. R. (2020). Chronostratigraphy, site formation, and palaeoenvironmental context of late pleistocene and holocene occupations at grassridge rock shelter (Eastern Cape, South Africa). Open Quaternary, 6 (1), 1-19.

Authors

Christopher J.H. Ames, Luke A. Gliganic, Carlos Cordova, Kelsey Boyd, Brian G. Jones, Lisa Maher, and Benjamin Collins

OPENQUATERNARY

Ames, CJH, et al. 2020. Chronostratigraphy, Site Formation, and Palaeoenvironmental Context of Late Pleistocene and Holocene Occupations at Grassridge Rock Shelter (Eastern Cape, South Africa). *Open Quaternary*, 6: 5, pp. 1–19. DOI: https://doi.org/10.5334/oq.77

RESEARCH PAPER

Chronostratigraphy, Site Formation, and Palaeoenvironmental Context of Late Pleistocene and Holocene Occupations at Grassridge Rock Shelter (Eastern Cape, South Africa)

Christopher J. H. Ames[*,†], Luke Gliganic[‡], Carlos E. Cordova[§], Kelsey Boyd[*], Brian G. Jones[*], Lisa Maher[‖] and B. R. Collins[¶,**]

Grassridge rock shelter is located in the high elevation grassland foothills of the Stormberg Mountains in the Eastern Cape of South Africa. This places Grassridge at an important biogeoclimatic intersection between the Drakensberg Mountains, the South African coastal zone, and the interior arid lands of southern Africa. First excavated in 1979, the approximately 1.5 m stratigraphic sequence was divided into two major occupational components: a 50–70 cm thick Later Stone Age component dating between 7–6 ka and an underlying 50–80 cm thick Middle Stone Age component dated to 36 ka at the base. Here we present a reanalysis of the Grassridge stratigraphic sequence that combines new optically stimulated luminescence and radiocarbon age estimates with sedimentological and microbotanical analyses to evaluate site formation processes and the palaeoenvironmental context of human occupations. Results indicate a complex history of geogenic, anthropogenic, and biogenic inputs to the depositional sequence that are interspersed with pulsed human occupation from 43–28 ka, 13.5–11.6 ka, and 7.3–6.8 ka. Microbotanical remains indicate a cooler, drier grassland environment in MIS 3 that transitions to a warmer, moister grassland environment dominated by summer rainfall in the middle of MIS 1. The pulsed occupational sequence identified at Grassridge is characteristic of the Pleistocene and Holocene record across the greater high elevation grassland region of South Africa, which, based on comparison with other currently available evidence, seems linked to a complex system of forager mobility entwined with rapidly fluctuating palaeoenvironments across the last glacial to interglacial transition.

Keywords: Geoarchaeology; South Africa; Eastern Cape; Phytoliths; Site Formation; MIS 3; MIS 1; Younger Dryas

1. Introduction

There is a rich tradition of Pleistocene archaeological research in southern Africa, which over the past century has significantly contributed to our understanding of human origins (Barham & Mitchell 2008). The distribution of this research, however, is not uniform throughout the region. A majority of what we know about Pleistocene human lifeways derives from well-studied rock shelter sites on or near the coastal margins (see Lombard et al., 2012). Inland sites are less frequent in this body of work and cluster in a few areas: the Drakensberg Highlands (Mitchell 1996; Plug & Mitchel 2008; Stewart et al. 2012; Wadley 1997), the Cradle of Humankind near Johannesburg (Kuman et al. 2018; Pickering et al. 2018; Riga et al. 2019), the Cederberg Mountains in the Western Cape (Hallinan & Parkington 2017; Lin, Douglass & Mackay 2016; Mackay et al. 2014; Shaw et al. 2019), and the central portion of the Orange River (Sampson 1972, 1970, 1968; Sampson et al. 2015). Yet at the macro-scale, and particularly for the Pleistocene record, there are large gaps in the distribution of recorded archaeological sites—most notable is the absence of data from the arid central interior, including the Nama-Karoo, northern savannah regions, and north-

* Centre for Archaeological Science, University of Wollongong, AU
† Department of Anthropology, University of Victoria, CA
‡ Institute of Geology, University of Innsbruck, AT
§ Department of Geography, Oklahoma State University, US
‖ Department of Anthropology, University of California-Berkeley, US
¶ Department of Anthropology, University of Manitoba, CA
** Department of Archaeology, University of Cape Town, ZA
Corresponding author: Christopher J. H. Ames (cames@uow.edu.au)

central dry highland grasslands. Some have argued that the absence or the differing nature of the data from these regions suggests it was ephemeral in the prehistory of southern Africa, with the coastal zone hypothesized as a critical region of occupation and potential driver of human evolution (Fisher et al. 2013; Marean 2016, 2014). However, the few well-described inland sites scattered across these interior regions, such as Kathu Pan (Lukich et al. 2019) and Wonderwerk (Chazan 2015; Chazan et al. 2008; Ecker et al. 2017), or the density of open sites in the Zeekoe Valley (Sampson et al. 2015), hint to a rich and deep-time record of human habitation in the interior. Continued exploration is required to understand the nature and sequence of occupation and adaptation in the inland areas of southern Africa, and to clarify the relationships between foragers in the interior and the coastal regions.

The Grassridge Archaeological and Palaeoenvironmental Project (GAPP) was initiated to address such questions, with a particular focus on the high altitude grasslands of the Stormberg Mountains in the Eastern Cape of South Africa (Collins, Wilkins & Ames 2017). Previous research in this area has focused primarily on Holocene-aged occupations and rock art, while only generally documenting the presence of Late Pleistocene archaeology (Deacon 1976; Opperman 1988, 1987, 1984; Sampson 1970). This leaves human occupation in the Stormberg region during the Late Pleistocene poorly understood, with overall limited research on the topic and an archaeological record defined by poorly resolved occupational pulses. Our ongoing work at Grassridge rock shelter is an initial step in evaluating the nature of these occupational pulses, and aims to shed light on the nature of adaptation and mobility in the highland grasslands. This research also provides a starting point for comparisons of Pleistocene and Holocene lifeways across the coastal, montane, and arid central interior regions of southern Africa—ultimately contributing to our understanding of socio-cultural networks across biogeoclimatic zones and their relationship to palaeoenvironmental changes through time.

In this paper, we present the chronostratigraphic framework for Grassridge along with characterisation of the sedimentary sequence. The objective is to integrate biogenic silica microfossil data, particularly from phytoliths, with stratigraphic, geochronological, and sedimentological data to discuss the anthropogenic, geogenic, and biogenic contributions to site formation, as well as the palaeoenvironmental context of the Late Pleistocene and Holocene occupational sequence.

2. Grassridge Rock Shelter and the Stormberg Region

Grassridge rock shelter is located 1500 metres above mean sea level (masl) in the grassland foothills of the Stormberg Mountains in the Eastern Cape of South Africa (**Figure 1**).

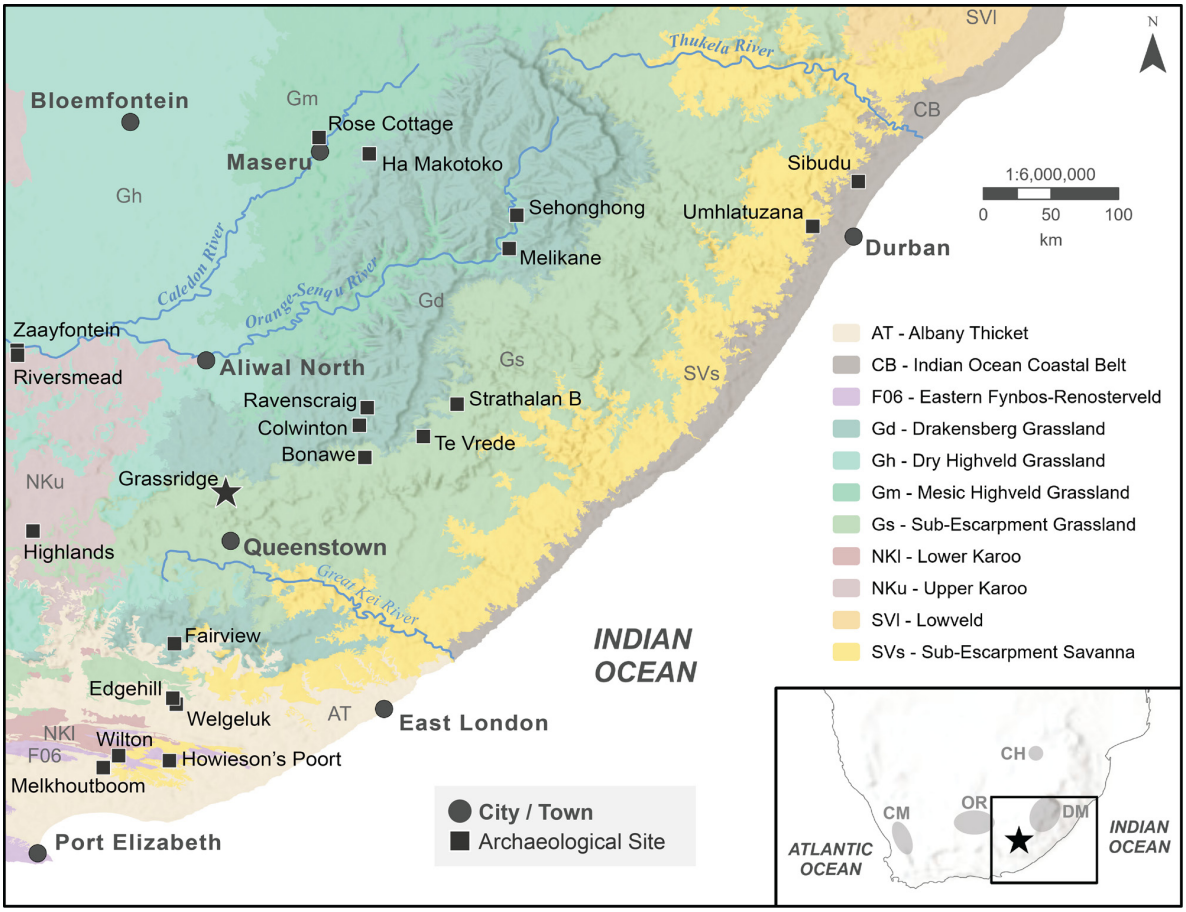

Figure 1: Grassridge shelter (star) and relevant other archaeological sites in relation to modern vegetation bioregions (Mucina & Rutherford 2006); the inset shows the approximate locations of the Drakensberg Mountains (DM), the Orange River Scheme area (OR), the Cederberg Mountains (CM), and the Cradle of Humankind (CH). Figure produced by Christopher Ames.

Situated approximately 200 km from the Indian Ocean coastline, the Stormberg region is the southwestern extent of the Grassland biome, and close to intersections with the Nama-Karoo biome, a variety of coastal biomes to the south and southeast, as well as the Drakensberg Mountains to the northeast. The area receives 400–600 mm/year of precipitation, which falls primarily in austral summer from October–May. Temperatures exceed 30°C in summer and regularly drop below freezing in winter with frequent frosts (Hoare & Bredenkamp 2001; Opperman 1987; Sampson 1970). Elevation increases from southwest to northeast across the region, from approximately 1200–1800 masl, and is positively correlated with rainfall and negatively correlated with temperature (Hoare & Bredenkamp 2001).

Grassridge is a large, curving shelter scoured into the western rock face at the top end of a small steep-sided valley (**Figure 2**). The shelter faces southeast with an opening approximately 40 m wide and is 10 m deep from the dripline to back wall. The height varies from 6–7 m at the dripline but narrows to less than 1 m at the back wall. Small quantities of water currently seep into some areas at the back of the shelter, as well as dripping from the roof in isolated areas. The curving nature of the shelter suggests it formed by water scouring an alcove into weaker strata of the Clarens Formation (Grab 2015; Castro & Bell 1995; Kitching & Raath 1984), which is a Triassic sandstone that along with the underlying Molteno and Elliot Formations represent the Stormberg Group (Karoo Supergroup) characteristic of the regional geology (Bordy & Catuneanu 2002; Bordy & Eriksson 2015; Smith 1990). Dolerite outcrops regularly cap this sequence across the landscape, formed by intrusive Jurassic dykes, sills, and inclined sheets (Chevallier & Woodford 1999; Coetzee & Kisters 2016). The dolerite intrusion is archaeologically relevant, as contact metamorphism created large quantities of hornfels (Aarnes et al. 2011)—a common raw material used for manufacturing stone tools in the local Middle and Later Stone Age sequence (Collins, Wilkins & Ames 2017; Opperman 1987).

The Stormberg Mountains emerge from the neighbouring plains to the south and west at roughly 1200 masl and encompasses the divide between the Orange River and Great Kei River watersheds. Tributaries in the southern Stormberg form the headwaters of the Black and White Kei Rivers, which merge into the Great Kei approximately 80 km southeast of Grassridge. The Stormberg Plateau and gentler northern slopes primarily drain northward into the Crow (*Kraai*) River—a substantial tributary that meets the Orange River east of Aliwal North. Grassridge is located at the upper reaches of the White Kei River along the Grootvleispruit drainage, and is less than 20 km from the divide with the Orange River watershed.

Following the classification of Mucina and Rutherford (2006), the high altitude plateau in the northern Stormberg is part of the Drakensberg Grassland bioregion consisting predominantly of the Stormberg Plateau Grassland with patches of the Southern Drakensberg Highland Grassland increasing in frequency to the east as elevation and rainfall increase. The former vegetation type occurs on the flat to undulating landscapes above ~1500 masl and is represented by grassland with a strong dwarf shrub component, whereas the latter is characterised by dense tussock grasslands on the highest mountain peaks and ridges. Although C_4 grasses dominate the Stormberg region, the higher elevations sustain many C_3 grasses (e.g., *Koeleria capensis, Merxmuellera disticha, M. drakensbergensis, Helictotrichon turgidulum* and *Pentaschistis microphylla*).

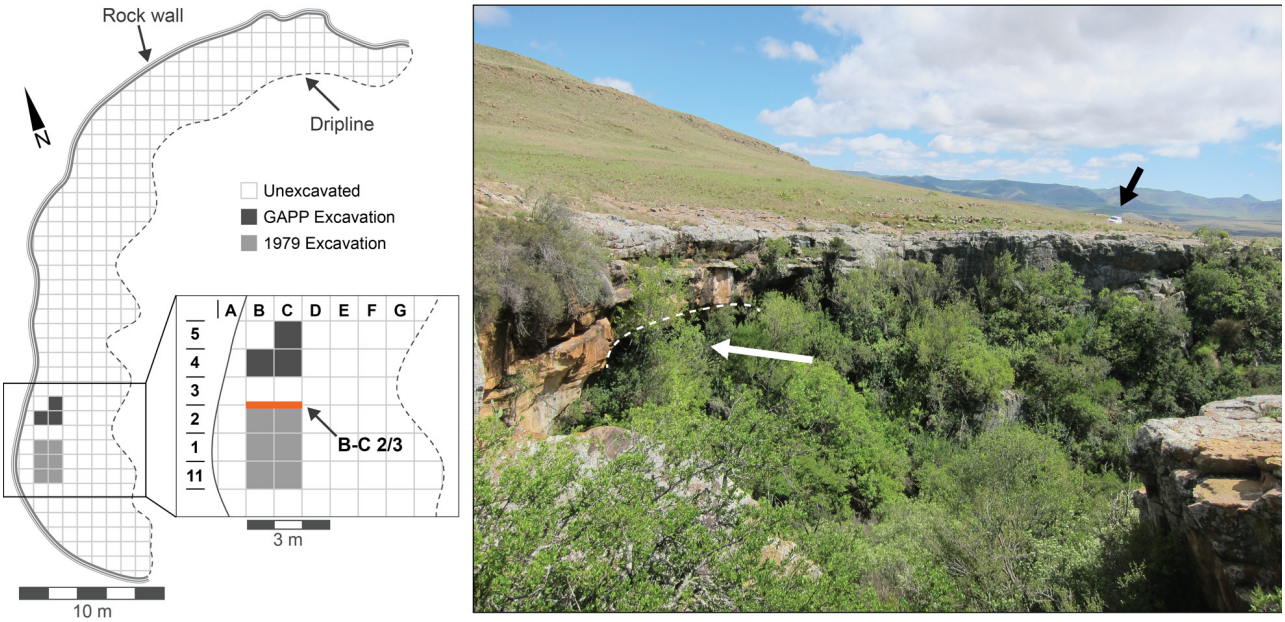

Figure 2: Plan of Grassridge shelter identifying the location of profile B-C 2/3 (bold orange line) and a photo of Grassridge shelter looking to the north; the dashed white line is the approximate location of the overhang and the white arrow points to the opening behind the vegetation (note vehicle—black arrow). Figure produced by Christopher Ames. Photo credit: GAPP 2014.

The southern portion of the Stormberg, where Grassridge is located, lies within the Sub-Escarpment Grassland bioregion. Here, gently undulating plains between 760–1580 masl consist of grassland to open thornveld dominated by the grass genera *Cymbopogon*, *Elionurus*, *Ergagrostis*, *Artistida*, and *Themeda*—known as the Tsomo Grassland. Non-grass vegetation includes herbs of the Asteraceae family (e.g., *Aster bakerianus* and *Berkheya onoparioides*) and a number of shrubs (e.g., *Felicia muricata*, *Senecio burchelli*, and *Euryops fluribundus*). Hillslopes and more moderate elevation ridges and hills, particularly those impacted by dolerite intrusion, are classified as Tarkastad Montane Shrubland (Mucina & Rutherford 2006), which consists of low, semi-open mixed shrubland. Small trees and shrubs are common here (e.g., *Acacia karoo*, *Cadaba aphylla*, *Dyospiros austroafricana, Tarchonanthus minor*, and *Rhus burchelli*), as well as a number of succulents (e.g., *Aloe ferox*) and C_4 grasses. Grassridge is within the Tarkastad Montane Shrubland in close proximity to the Tsomo Grassland, which dominates the surrounding undulating plains and valley bottoms.

To the south and southeast of Grassridge there are short-distance changes in grassland type, which are correlated with elevation and temperature, and influenced by the west to east increase in rainfall. Moreover, within 50 km to the northwest and southeast of the rock shelter the landscape transitions into Nama-Karoo and coastal Savanna biomes respectively. Grassridge is thus located at an important biogeoclimatic intersection and the local vegetation community would have been sensitive to palaeoenvironmental change.

3. Previous Research at Grassridge

Grassridge was initially excavated in 1979 (Opperman 1988, 1984). This work was conducted as part of a larger study of Later Stone Age (LSA) occupation in the Drakensberg region (Opperman 1987), and the primary study area was ~100 km to the east, with excavations at Ravenscraig, Colwinton, Te Vrede, and Bonawe rock shelters. The aim was to evaluate changes in subsistence practices along an altitudinal gradient between the Drakensberg Mountains and foothills. Grassridge was considered a comparative control sample located in a separate environment.

The original excavation at Grassridge consisted of a 2 × 3 m trench near the back wall in the southwest portion of the shelter (**Figure 2**). Opperman separated the 1.5 m stratigraphic sequence into two major components: a 50–70 cm thick LSA component divided into five occupational layers dating from 7–6 ka, and an underlying 50–80 cm thick Middle Stone Age (MSA) component divided into three occupational layers attributed to the Late Pleistocene by a single date of roughly 36 ka near bedrock (**Figure 3**). Although he noted there were no culturally sterile layers in the sequence, he argued there was a break between the MSA and LSA indicated by the compact nature of the MSA sediment compared to the loose, ashy LSA sediment. Opperman hypothesized that the shelter was uninhabited for thousands of years across this boundary during the Last Glacial Maximum (LGM) (Opperman 1987).

Nearly 10,000 stone artefacts were recovered from the MSA occupation layers (KGS, VGS, and GS), as well as a small assemblage of well-preserved faunal material that included the occasional fragment of ostrich eggshell (Opperman 1988). The stone artefacts—dominated by plain platform, unmodified hornfels flakes and blades—were typologically and metrically similar across all three layers. The small retouched piece component consisted of laterally retouched blades, points, scrapers, and retouched flakes. Twelve cores were recovered, but no technological detail is provided. The total minimum number of individuals reported for the faunal assemblage is only 15, but the data hints to a preference for medium to large antelope species such as hartebeest and wildebeest (Opperman 1988).

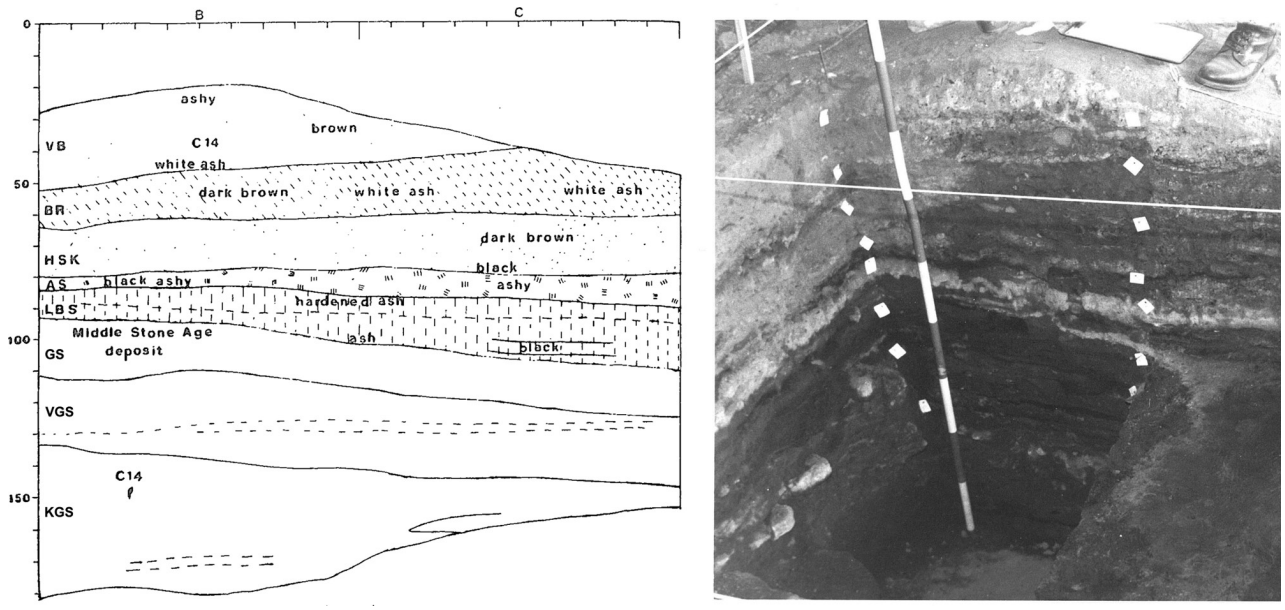

Figure 3: Stratigraphic drawing (scale in cm; modified from Opperman 1984: Figure 3) and photo of the B-C 2/3 profile from the 1979 Excavation at Grassridge. Photo credit: H. Opperman 1979; reproduced with permission.

The five LSA layers (LBS, AS, HSK, BR, and VB) produced large quantities of stone artefacts and faunal remains, along with some modified bone and shell objects (Opperman 1987, 1984). Relative to other sites in the neighbouring grassland regions, Grassridge produced significant quantities of ostrich eggshell (OES) beads, both complete and broken, as well as unmodified OES fragments. The presence of backed segments, small convex scrapers, and single platform cores suggests affiliation with the mid-Holocene Wilton technocomplex. There is some change in lithic technology throughout the LSA sequence, with the lower layers (LBS and AS) being characterised by larger, elongated side and end scrapers, and the upper layers (HSK, BR, and VB) containing shorter, broader end scrapers. In addition, the faunal assemblage indicates a change in subsistence strategy from predominantly medium-large antelope species in the lower layers to predominantly small-medium game species in the upper layers.

The GAPP team revisited the shelter in 2014 to relocate the original excavation, reanalyse the stratigraphic sequence, and initiate new excavations. Many of the broad patterns identified by Opperman for the LSA are being confirmed, as well as new discoveries such as perforated *Nassarius* shells—a marine species that indicates interaction with the coastal zone—and a previously unknown terminal Pleistocene occupation (Collins, Wilkins & Ames 2017). Analysis of the newly excavated MSA and LSA materials is ongoing and those results will be presented elsewhere. Here we focus on the findings of our chrono-stratigraphic reanalysis of the 1979 stratigraphic sequence, including a multi-proxy site formation analysis and palaeoenvironmental reconstruction of the occupational sequence.

4. Methods

4.1. Field recording and sampling

In 2014, the GAPP team identified the original excavation at Grassridge and removed all backfill. The northern stratigraphic section—profile B-C 2/3—was scraped clean and reanalysed in detail (**Figure 2**). The objective of this reanalysis was to identify the smallest macroscopically visible strata, which are referred to here as stratigraphic units (SUs). SUs were marked with tags pinned to the section and they represent sedimentological layers, soil horizons, and/or anthropogenic features. Photographs were taken of each SU and standard soil and sedimentological properties recorded (Schoenenberger et al. 2002). A new stratigraphic sketch was produced and all SU boundaries were documented using a total station referenced to the original 1979 excavation grid system. Bulk sediment samples were collected from all layers of sufficient thickness for laboratory characterisation and microbotanical analyses. Intact charcoal fragments were collected for radiocarbon dating when encountered, and the excavation trench was reopened in 2018 to collect a series of optically stimulated luminescence (OSL) dating samples. Based on laboratory and geochronological results, SUs are grouped into lithostratigraphic zones (LZs), which represent major geogenic or anthropogenic changes in the depositional history of Grassridge. This study focuses on the chronostratigraphic framework, palaeoenvironmental context, and site formation processes of the Grassridge LZs. SUs can be sub-divided into micro-facies through the analysis of thin sections (e.g., Miller et al., 2013), but the microstratigraphic analysis of the Grassridge sequence is ongoing and will be presented elsewhere.

4.2. Geochronology

Twelve intact individual charcoal fragments were sent for radiocarbon dating by accelerator mass spectrometry (AMS) to two different laboratories. Two samples were dated at Beta Analytic Inc. (Beta) and 10 samples were dated at the University of California Irvine (UCI), both in the USA. These 12 new ages are combined with previously published ^{14}C ages sampled from the B-C 2/3 stratigraphic sequence. Pre-existing ages include three obtained by GAPP from the Centre for Accelerator Mass Spectrometry (CAMS) in Berkeley, USA (Collins, Wilkins & Ames 2017), and two dates from the Pretoria laboratory in South Africa obtained by Opperman following the 1979 excavation (Opperman 1984). All 17 radiocarbon ages were calibrated in OxCal 4.3 (Bronk Ramsey & Lee 2013) using the SHCal13 calibration curve (Hogg et al. 2013).

Eight samples were processed for single-grain OSL dating to establish the age of the lowermost deposits, and to provide an independent comparison with the radiocarbon results that were anticipated to approach the practical limit of the technique. OSL samples were collected from the lower two-thirds of the B-C 2/3 profile in 2018 by hammering 4 cm diameter opaque stainless steel tubes into the cleaned section. Quartz grains of 150–180 and 180–212 μm diameter were extracted from the sediment samples under dim red illumination using standard procedures (Gliganic et al. 2017; Wintle 1997). Equivalent dose (De) values were measured using the single-aliquot regenerative dose (SAR) procedure (Murray & Wintle 2000) with natural/regenerative dose and test doses of 220°C for 10 s and 200°C for 5 s, respectively. De distributions were modelled using the central age model (CAM; Galbraith et al. 1999) and the finite mixture model (FMM; Roberts et al. 2000) following Gliganic et al. (2015). Dose rates were estimated using a combination of GM-25-5 beta counting, thick source alpha counting, and cosmic dose rate calculation (Prescott & Hutton 1994). Additional details regarding measurement parameters, dose recovery experiments, statistical models, and dose rate measurements and calculations are provided as supplementary material (Supplementary file 1).

4.3. Sedimentological analyses

Bulk sediment samples were first sieved into coarse (>2 mm) and fine (<2 mm) fractions. Coarse fractions were sorted into charcoal, cultural (i.e., stone artefacts, faunal remains, ochreous rock), and non-cultural components and weighed. Fine fractions were sub-sampled for pH determination, loss-on-ignition, grain size measurement, and mineralogical characterisation. Soil pH was measured in water by electronic metre using a sediment to water ratio of 1:2 (Hendershot, Lalande &

Duquette 1993). Organic carbon content was estimated using loss-on-ignition (LOI) following the methods outlined in Dean (1974), Heiri et al. (2001), and Santisteban et al. (2004). One gram of oven-dried sample (105°C for 12 hours) was combusted in a muffle furnace at 550°C for four hours; the percentage weight loss is proportional to the organic carbon content. Mineralogical characterisation of the samples was achieved with x-ray diffraction (XRD). One gram sub-samples were ground into powder using an agate mortar and pestle and then analysed with a GBC MMA x-ray diffractometer with solid state detector. Peaks in the resulting spectra were identified using TRACES and analysed using SIROQUANT software to establish the relative volumetric proportions of the different minerals present. Lastly, one gram sub-samples were taken for grain size analysis and treated with 10% HCl to remove carbonates, followed by successive cold and heated 30% H_2O_2 treatments to remove organic matter (Sheldrick & Wang 1993). Particle size distributions were determined for the pre-treated samples using a Malvern Mastersizer 2000 with active sonication—distributions were produced in triplicate for each sample and an average distribution calculated.

4.4. Microbotanical analysis

Biogenic silica microfossils were extracted from approximately 15 g of bulk sediment fine fraction. Sample extraction procedures follow those of Joines (2011), which combines aspects discussed in Lentfer & Boyd (1998) and Zhao & Pearsall (1998). Samples were first sieved through 125 μm mesh and 1 g of the <125 μm fraction was treated with 30% HCl to remove carbonates. The carbonate-free samples were washed for 10 seconds in 10% KOH, and then clays were deflocculated by adding a 0.5% solution of $NaPO_3$. Samples were neutralised with deionized water, centrifuged, and the supernatant decanted between all steps. Finally, biogenic silica microfossils were isolated by flotation using a heavy-liquid solution of sodium polytungstate (2.3 $g{\cdot}cm^{-3}$) and extracted from the sample supernatant by pipette, oven dried, and mounted on microscope slides using Canada balsam for identification and counting.

Results of the biogenic silica extractions are presented in summary format and include overall proportions of phytoliths, diatoms, and sponge spicules (Supplementary file 3). Taphonomic indicators are also provided, including the proportion of damaged phytoliths, the concentration of recovered phytoliths per gram of sediment, and the abundance of husk phytoliths. The first category relates to preservation, whereas the latter two are indicative of anthropogenic contributions such as intensity of occupation and the storage or processing of seeds or grain respectively (Piperno 2006). Phytolith morphotypes are examined in further detail, focusing on key ratios of palaeoecological and palaeoclimatic significance. These include the ratio of graminoids (e.g., grasses and sedges) to non-graminoids (i.e., dicots), woody (ligneous dicotyledon) plants to grasses (Poaceae), C_3 to C_4 diagnostic grass silica short cells (GSSCs), and the more mesic Panicoideae C_4 GSSCs to the more drought-resistant Chloridoideae C_4 GSSCs (Supplementary file 3). Biogenic silica and sedimentological data are plotted using C_2 Version 1.7.7 software (Juggins 2014).

5. Results

5.1. The Grassridge stratigraphic sequence

Stratigraphic reanalysis of units B and C along the 2/3 line (**Figure 2**) allows comparison with the published 1979 stratigraphic divisions (Opperman 1984). Other than collapsed corners, the profile was in good condition and many observed features could be matched to the original sketch, such as ashy patches and charcoal-rich lenses. No wall tags remained from the 1979 excavation, but by comparison with historical photographs, the original sketch, and sedimentary descriptions (Opperman 1988, 1987, 1984), it was possible to identify the approximate boundaries of the 1979 stratigraphic divisions (**Figure 4**).

The GAPP stratigraphic reanalysis identified finer layering in the sequence than previously reported (**Figure 5**). Moreover, we identified a sharp discontinuity in the sequence signalled by a sloping carbonate crust that splits the profile into a lower and upper sequence. These two LZs have been previously noted in the Grassridge sequence and referred to as Zones II and I respectively (Collins, Wilkins & Ames 2017). For this study, Zone I has been further divided into two zones. To maintain consistency with previously published terminology these new divisions are referred to as Zones Ib and Ia, although they are distinct and should not be viewed as sub-divisions.

LZ II consists of 23 individual SUs and is characterised by 45–85 cm of yellowish brown to dark yellowish brown silty sands and sandy silts supporting relatively high quantities of medium to coarse sandstone gravels. Stone tools are visible in the profile throughout LZ II and there are multiple charcoal-rich stringers and lenses. A wedge-shaped mass of very coarse sandstone gravels and medium-sized mudstone boulders (SUs 40 and 43) is present in the lower left, which sandwich two thin layers of sediment and charcoal (SUs 41 and 42). This entire LZ is capped by a thin, weakly laminated carbonate crust (SU 29).

LZs Ib and Ia are noticeably richer in cultural remains than LZ II. Zone Ib is only 5–10 cm thick, comprising five SUs that rest uncomformably atop LZ II. The only SU to extend laterally across the entire LZ Ib sequence is a yellowish brown to dark yellowish brown silty sand with low quantities of fine gravel (SU 25). There is also a sharply defined light grey to pale brown homogeneous ash feature (SU 23) interdigitated with and overlying a series of charcoal-rich lenses (SUs 22, 24, 26).

An abrupt transition separates LZ Ib from LZ Ia. Zone Ia contains 21 SUs and comprises 35–60 cm of deposit. The sediments consist predominantly of thick, light greyish brown to pale brown sandy silts to silty sands (SUs 1, 2, 4–6, 8, 10, 14, 16–18, 20, and 21). These deposits are ashy and contain abundant scattered charcoal pieces, burnt and calcined bone fragments, and stone artefacts. Regular thin layers of reddish brown to dark brown sediment transect these ashy deposits (SUs 3, 7, 9, 11, and 19), and there is a clearly defined thick lens of pale brown to light grey homogeneous

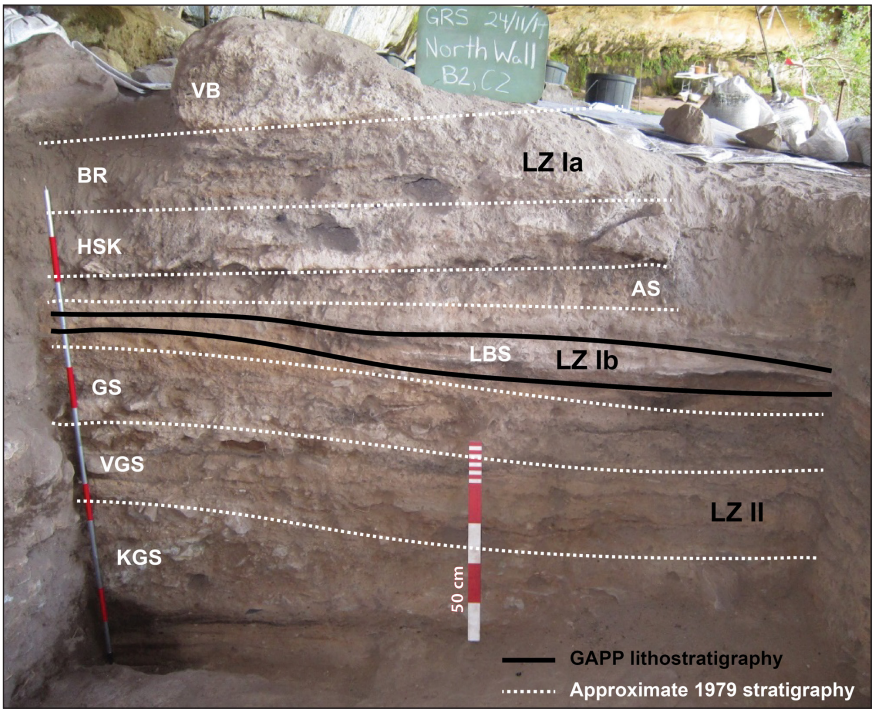

Figure 4: Photograph of the B-C 2/3 stratigraphic sequence with overlay of 1979 divisions and GAPP lithostratigraphic zones (large red segments of scale bars are 10 cm). Figure produced by Christopher Ames. Photo credit: GAPP 2014.

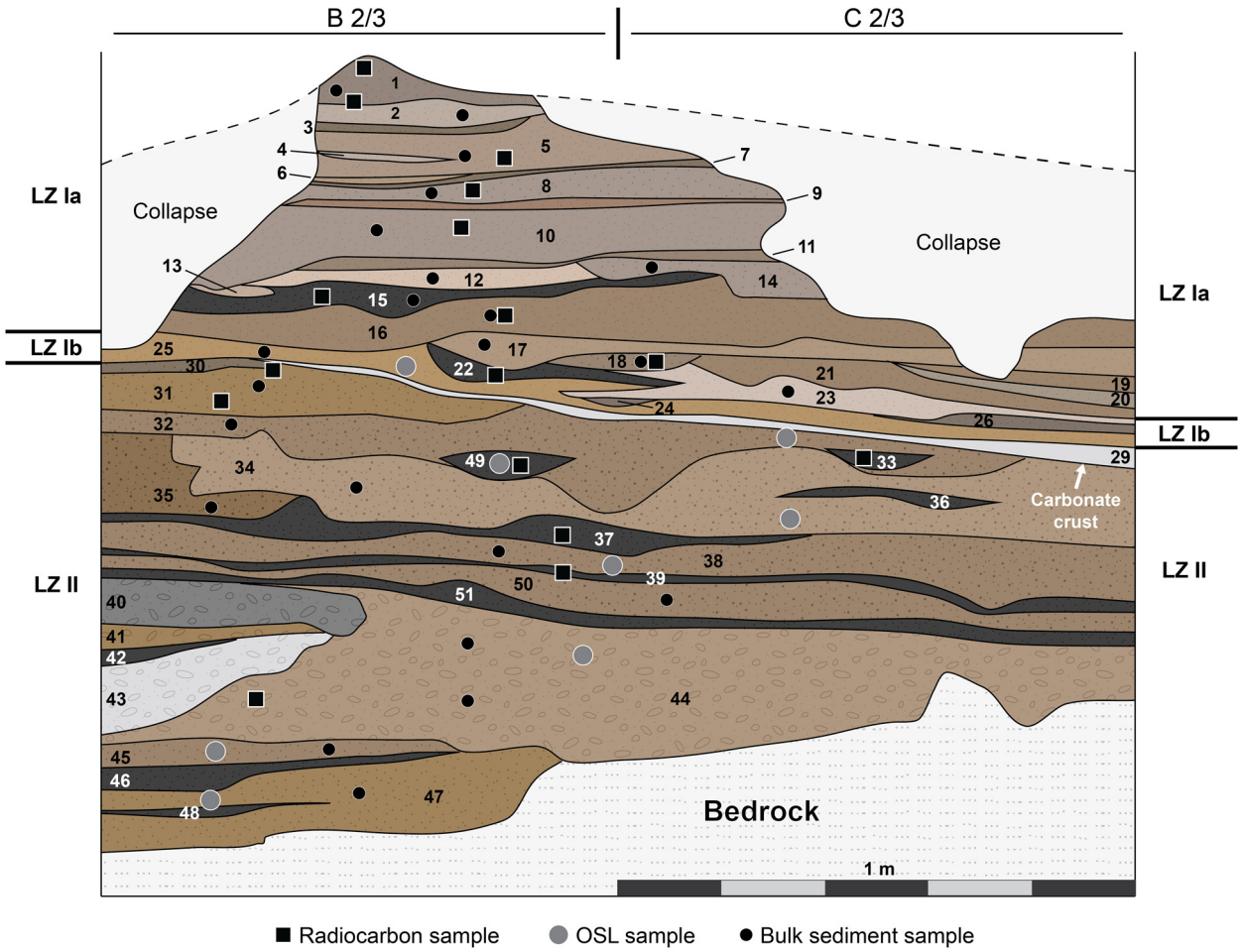

Figure 5: GAPP stratigraphic drawing of the B-C 2/3 profile showing numbered stratigraphic units, lithostratigraphic zones, and sample locations. Figure produced by Christopher Ames.

Table 1: Stratigraphic descriptions following the 1979 excavation (Opperman 1988, 1987, 1984) in relation to the lithostratigraphic zones defined during reanalysis (see Supplementary file 2 for more detail).

1979 Stratigraphic Divisions		GAPP Stratigraphic Units	GAPP Lithostratigraphic Zones	
VB	Compact brown ashy loam	1, 2, 3	Ia	A sequence of horizontal fine sandy silts, alternating between 5–10 cm thick layers of grey, ashy, artefact-rich sediment and thin (1–3 cm) rubefied layers. Individual layer boundaries are clear to gradual. Within this zone is a 2–5 cm thick massive, creamy white ash layer that sits atop a 3–5 cm thick loose, charcoal-rich layer. The lower boundary of the zone is abrupt. Artefacts are abundant throughout, including lithics, ochre, and shell, but dominated by burnt and calcined bone fragments.
BR	Loose very dark sandy loam mixed with patches of white ash	5, 4, 6, 7, 8, 9		
HSK	Dark brown sand with abundant faunal remains, lithics, and charcoal with the highest frequency of formal tools	10, 11, 14, 12, 13		
AS	Thin layer of loose, fine, ashy sands with greater artefact frequency than LBS	15 and part of 16		
LBS	Dark brown to black fine sandy layer with the top and bottom consisting of hardened ash horizons and containing relatively little cultural material	part of 16 and 17, 18, 19, 20, 21		
		22, 23, 24, 26, 25	Ib	A thin horizontal yellowish brown fine sandy silt layer containing a 1–5 cm thick and 1 m wide deposit of massive, creamy white ash intercalated with a charcoal-rich lens. Rubification of the fine sandy silts underlying this combustion feature is noted. The lower boundary slopes toward the dripline and is demarcated by an unconformity. All artefact types are present, but in lower frequency than the overlying zone.
		29, 30, 33 and part of 31, 32, 34	II	Gently sloping dark brown to dark yellowish brown silty fine sands supporting frequent small to medium size gravels. The top of the sequence is marked by a 1–3 cm thick carbonate crust, which is weakly laminated and thickest toward the dripline. Charcoal-rich stringers (1–3 cm thick) are common, with some spanning the width of the profile. Multiple clearly defined charcoal-rich lenses are also present, and there is a wedge of deposit with more common and larger gravels at the western edge of the profile. The base of the sequence rests on bedrock. Stone artefacts occur in similar frequency as the overlying zone, but faunal remains are extremely rare.
GS	Compact brown sand with much higher frequency of lithics than the underlying layers, but bone fragments are rare	Part of 31, 32, 34, and 49, 36, 35		
VGS	Light brown sand with similar cultural remains as KGS, but fewer bone fragments	37, 38, 39, 50, 51		
KGS	Hardened brown sand overlying bedrock containing lithics, charcoal pieces, and bone fragments	40, 41, 42, 43, 44, 45, 46, 47, 48		

ash (SU 13) that caps a thin, loose, dark brown to black silty loam (SU 15) in the lower third of the LZ.

Comparing the 1979 boundaries with the stratigraphic reanalysis shows that the AS-LBS boundary sits slightly above the Zone Ib-Ia boundary (**Table 1**; **Figure 4**). There is also some uncertainty regarding how the Zone II-Ib boundary corresponds to the 1979 stratigraphic divisions. In the original B-C 2/3 drawing, a hardened ash layer cuts through the approximate centre of LBS. Opperman's description of the hardened ash feature is most consistent with the carbonate crust capping Zone II (Opperman 1987). Moreover, the black lens marked in the lower right-hand portion of LBS on the original sketch (see **Figure 3**) aligns with a distinct charcoal-rich lens visible in the profile photo (**Figure 4**). Together, this evidence suggests that the LBS lower boundary defined in 1979 may cross the profile slightly below the carbonate crust that marks the Zone II-Ib boundary in the revised scheme.

5.2. Geochronological results

5.2.1. Radiocarbon ages

Of the twelve new radiocarbon ages, five are from LZ II and seven fall within LZ Ia (**Table 2**). The oldest mean age is 39.2k cal a BP from SU 39 (UCI-209050) and the youngest is 6.81k cal a BP from SU 1 (UCI-209041) only a few centimetres below the surface. Although not a linear age-depth sequence, all twelve mean ages are in stratigraphic order except for the samples from SU 16 and 18—7.36k cal a BP and 7.24k cal a BP respectively. Yet, these two ages do overlap at the 2σ confidence interval and should be considered coincident. The three previously published Holocene ages of 7.06k cal a BP (CAMS-170784), 7.92k cal a BP (Pta-2970), and 11.6k cal a BP (CAMS-170783) are in line with the expanded chronological sequence, as is the 45.3–35.1k cal a BP date (CAMS-169741) when considering the large confidence interval. The radiocarbon age of 42.4–39.4k cal a BP (Pta-2714) originally reported

Table 2: Conventional and calibrated ^{14}C age estimates on charcoal from the B-C 2/3 sequence (LZ = lithostratigraphic zone; SU = stratigraphic unit). Age calibrations with OxCal v 4.2.3 (Bronk Ramsey & Lee 2013) using the SHCal13 (Hogg et al. 2013) calibration curve.

Sample Code	GAPP LZ	GAPP SU	1979 Layer	Conventional ^{14}C a BP	k cal a BP (95.4%)	*x* age k cal a BP	Reference
UCI-209041	Ia	1	VB*	6015 ± 15	6.89–6.74	6.81	this paper
UCI-209042	Ia	1	VB*	6040 ± 15	6.91–6.75	6.84	this paper
Pta-2970	Ia	3*	VB	6090 ± 80	7.16–6.72	6.92	Opperman, 1984
UCI-209043	Ia	5	BR*	6085 ± 15	6.96–6.80	6.89	this paper
UCI-209044	Ia	8	BR*	6100 ± 15	6.99–6.80	6.91	this paper
CAMS-170784	Ia	10	HSK*	6200 ± 35	7.17–6.94	7.06	Collins et al., 2017
UCI-209045	Ia	15	HSK*	6355 ± 25	7.31–7.17	7.23	this paper
Beta-532051	Ia	16	AS*	6470 ± 30	7.42–7.23	7.36	this paper
Beta-532052	Ia	18	AS*	6360 ± 30	7.32–7.17	7.24	this paper
CAMS-170783	Ib	22	LBS*	10125 ± 50	12.0–11.4	11.6	Collins et al., 2017
UCI-209046	II	30	LBS*	24170 ± 190	28.6–27.8	28.2	this paper
UCI-209047	II	31	LBS*	32120 ± 240	36.5–35.4	36.0	this paper
UCI-209048	II	49	GS*	32710 ± 260	37.6–36.0	36.7	this paper
UCI-209049	II	37	VGS*	33830 ± 300	38.9–37.2	38.2	this paper
UCI-209050	II	39	VGS*	34720 ± 330	40.0–38.5	39.2	this paper
CAMS-169741	II	33	LBS*	35000 ± 2200	45.3–35.1	40.0	Collins et al., 2017
Pta-2714	II	44	KGS	36380 ± 870	42.4–39.4	40.9	Opperman, 1984

* Best approximation based on the identification of Opperman's layers during stratigraphic reanalysis.

from near the base of the B/C 2–3 sequence is older and stratigraphically below all other ^{14}C samples. In conjunction with the OSL results below, there is justification for accepting the date as valid despite it approaching the practical limit of radiocarbon dating.

5.2.2. Optically stimulated luminescence ages

Single-grain dose recovery experiments were performed using sample GRS 6. Grains were bleached with blue LEDs for 100 s twice before given a surrogate natural dose of 46 Gy in the Risø TL/OSL reader. The measured/given dose ratio of 1.05 ± 0.03 with 0% overdispersion is consistent with unity at 2σ, indicating that the SAR procedure is appropriate for estimating known radiation doses.

Eight OSL samples were processed from the lower two-thirds of the stratigraphic sequence (**Tables 3** and **4**). One sample is from LZ Ib, with the remaining seven spread across LZ II. As overdispersion values are generally high for all samples, only two were best fit by the FMM. The oldest OSL age is 43.1 ± 4.8 ka from SU 47 near bedrock, with the youngest OSL age of 13.5 ± 1.0 ka coming from SU 25 at the base of LZ Ib immediately

Table 3: Dose rate data for OSL samples from the B-C 2/3 sequence (see Supplementary file 1 for more detail).

Sample	Measured water content*	Gamma (Gy/ka)**	Beta (Gy/ka)	Cosmic (Gy/ka)	Total (Gy/ka)***
GRS 1	15.3	0.56 ± 0.02	0.89 ± 0.05	0.03 ± 0.00	1.51 ± 0.09
GRS 6	15.2	0.84 ± 0.02	1.31 ± 0.07	0.03 ± 0.00	2.21 ± 0.13
GRS 7	12.9	0.90 ± 0.02	1.36 ± 0.07	0.02 ± 0.00	2.32 ± 0.13
GRS 8	10.4	0.88 ± 0.02	1.43 ± 0.07	0.02 ± 0.00	2.36 ± 0.14
GRS 9	7.5	0.82 ± 0.03	1.15 ± 0.06	0.02 ± 0.00	2.02 ± 0.12
GRS 11	20.9	0.57 ± 0.01	0.90 ± 0.05	0.03 ± 0.00	1.53 ± 0.09
GRS 12	6.1	0.69 ± 0.02	1.07 ± 0.05	0.03 ± 0.00	1.82 ± 0.11
GRS 13	8.8	0.73 ± 0.02	1.14 ± 0.05	0.03 ± 0.00	1.92 ± 0.11

* Ages calculated using a water content of 12.1 ± 4.0%.
** GRS 9 gamma dose rate includes contribution from underlying bedrock (8 cm below).
*** Includes an internal contribution of 0.03 ± 0.01 Gy/ka.

Table 4: Equivalent dose and age data for OSL samples from the B-C 2/3 sequence. (LZ = lithostratigraphic zone; SU = stratigraphic unit)

Sample	GAPP LZ	GAPP SU	1979 Layer	Grain size (μm)	n=	OD (%)	Age Model	FMM OD	De (Gy)	Age (ka)
GRS 1	Ib	25	LBS	180–212	81	27 ± 4	CAM		20.3 ± 0.9	13.5 ± 1.0
GRS 12	II	32	LBS	150–180	168	49 ± 3	FMM, k = 2	38	57.6 ± 2.7	31.6 ± 2.5
GRS 13	II	34	GS	150–180	82	42 ± 5	CAM		65.9 ± 3.8	34.3 ± 2.9
GRS 6	II	38	VGS	180–212	69	50 ± 7	CAM		76.1 ± 6.5	34.4 ± 3.6
GRS 7	II	44	KGS	180–212	60	50 ± 9	CAM		81.9 ± 8.2	35.3 ± 4.1
GRS 8	II	45	KGS	150–180 + 180–212	84	45 ± 6	CAM		86.0 ± 6.1	36.4 ± 3.4
GRS 11	II	32/49	GS	150–180	144	34 ± 3	CAM		57.5 ± 1.9	37.6 ± 2.6
GRS 9	II	47	KGS	180–212	65	89 ± 10	FMM, k = 2	58	87.2 ± 8.0	43.1 ± 4.8

above the carbonate crust. All OSL ages are in chronological sequence and align well with the eight overlapping ^{14}C dates—both OSL and ^{14}C ages follow indistinguishable age-depth patterns and are statistically consistent at 1σ or 2σ (**Figure 6**; **Tables 2** and **3**).

5.3. Zone II sediments (approximately 43–28 ka)

OSL and radiocarbon dates indicate gradual deposition of Zone II between approximately 43 ka and 28 ka—a sedimentation rate of approximately 0.06 mm/year based on a maximum thickness of 85 cm and median ages. Sediments are slightly sandier in this LZ with notably higher coarse fractions (**Figure 6**). The proportion of gravel is highest in SU 44, which is the thickest unit of the entire sequence and the layer encasing the wedge of very coarse gravels and boulders. A similar pattern is observed for pH, with values of 8.3 at the bottom and top of LZ II, and higher values up to 8.8 in the centre of the zone. Other sedimentological variables have consistent values throughout the LZ, with changes primarily occurring near the uppermost boundary. Charcoal abundance, artefact concentration, organic carbon content, and the proportion of iron-bearing minerals all increase at this upper boundary, which is capped by a thin, weakly laminated calcium carbonate crust, while the >2 mm grain size content and the proportion of sand decrease over this time.

5.4. Zone Ib sediments (approximately 13.5–11.6 ka)

LZ Ib is restricted to only five SUs, only one of which (SU 25) crosses the entirety of the studied sequence (**Figure 5**). The other four SUs relate to interdigitated deposits indicative of combustion features (SUs 22, 23,

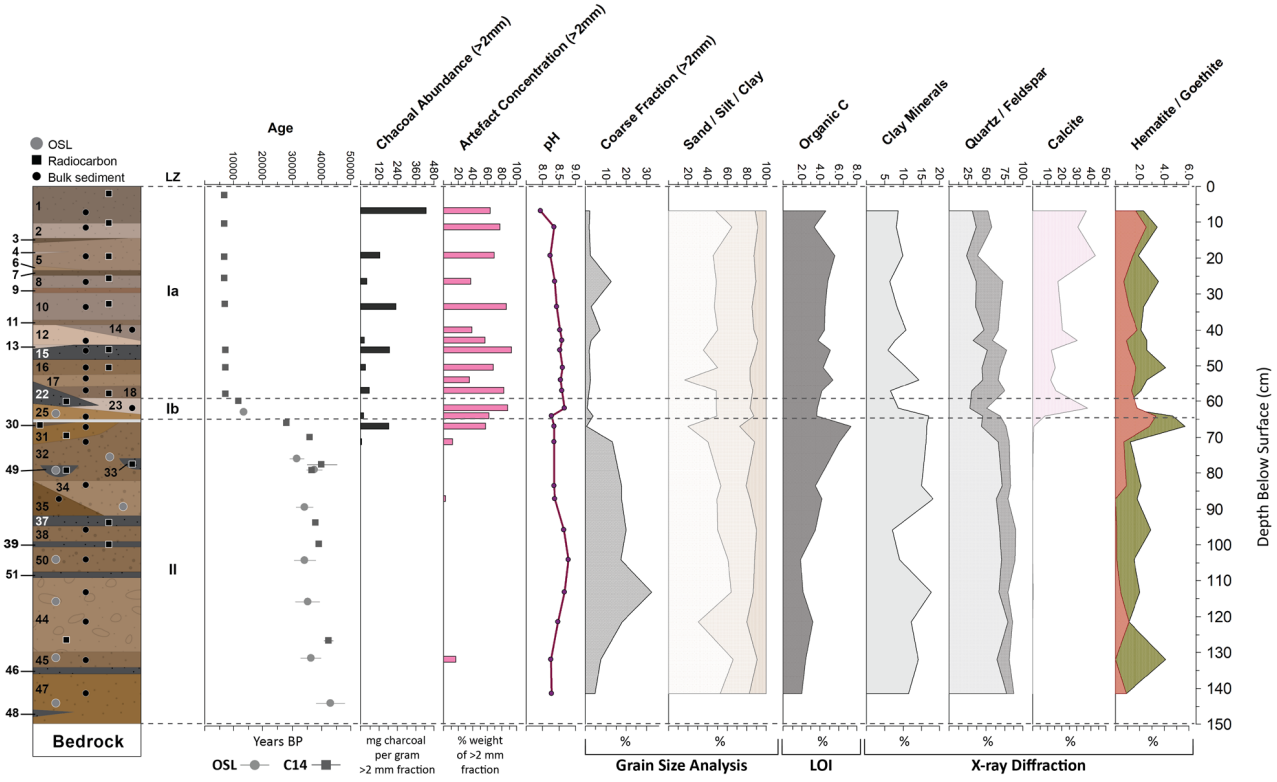

Figure 6: Schematic of the Grassridge sequence with geochronological results and sedimentological properties. Figure produced by Christopher Ames.

24, 26). Importantly, boundaries between the top of LZ Ib and the overlying sediments are all abrupt. The base of SU 25 dates to 13.5 ± 1.0 ka, whereas the overlying charcoal-rich lens (SU 22) that marks the top of the zone dates between 12.0–11.4k cal a BP. Using median ages and a maximum zone thickness of 10 cm, the sedimentation rate for LZ Ib is 0.05 mm/year. Despite a similar sedimentation rate to that determined for LZ II, the carbonate crust and overlying unconformity separating LZ II and Ib together represent approximately 15 kyr.

Only two bulk sediment samples from SU 25 and SU 23 were analysed from LZ Ib. There is relatively low charcoal abundance in their coarse fractions, but the artefact concentrations are relatively high. Both samples are silty sands with pH values of 8.3 and 8.7, and both contain small amounts of fine gravel. There is a pronounced decrease in iron oxide content from the yellowish brown SU 25 to the pale grey brown, ashy SU 23. Calcite content is notably higher than in the underlying layers, including a prominent peak associated with the homogeneous ash layer.

5.5. Zone Ia sediments (approximately 7.3–6.8 ka)

LZ Ia is unconformable with the underlying LZ Ib sediments. Charcoal from SU 18, which sits immediately on top of the 12.0–11.4k cal a BP charcoal-rich lens from LZ Ib, dates between 7.32–7.17k cal a BP. These dates indicate a 4–5 kyr unconformity between LZ Ib and Ia. At the top of LZ Ia, only 2.5 cm below the surface, charcoal from SU 1 dates between 6.89–6.74k cal a BP. Median ages plus a maximum thickness of 60 cm indicate accumulation of this zone over approximately 550 years, which is a relatively rapid sedimentation rate of 1.1 mm/year.

The sediments are rich in cultural remains—both charcoal and artefacts—and slightly finer than those in the underlying zones. Grain size distributions of the SUs hover at the boundary between sandy silts and silty sands, with the former being slightly more common. Fine gravels occur in low proportions throughout. The pH values gradually decline toward the surface, with values of 8.6 near the bottom of LZ Ia and 7.9 to 8.3 closer to the surface. Organic carbon and iron oxide contents are relatively stable throughout the zone, and calcite content increases toward the surface, from 12–15% at the base up to 31–40% at the top.

5.6. Phytoliths and other biogenic silica microfossils

Phytolith preservation is highly variable across the sequence, with the samples in LZ Ia and LZ Ib having the best preservation and consequently the higher concentrations (**Figure 7**). SU 17 in LZ Ia, however, did not have

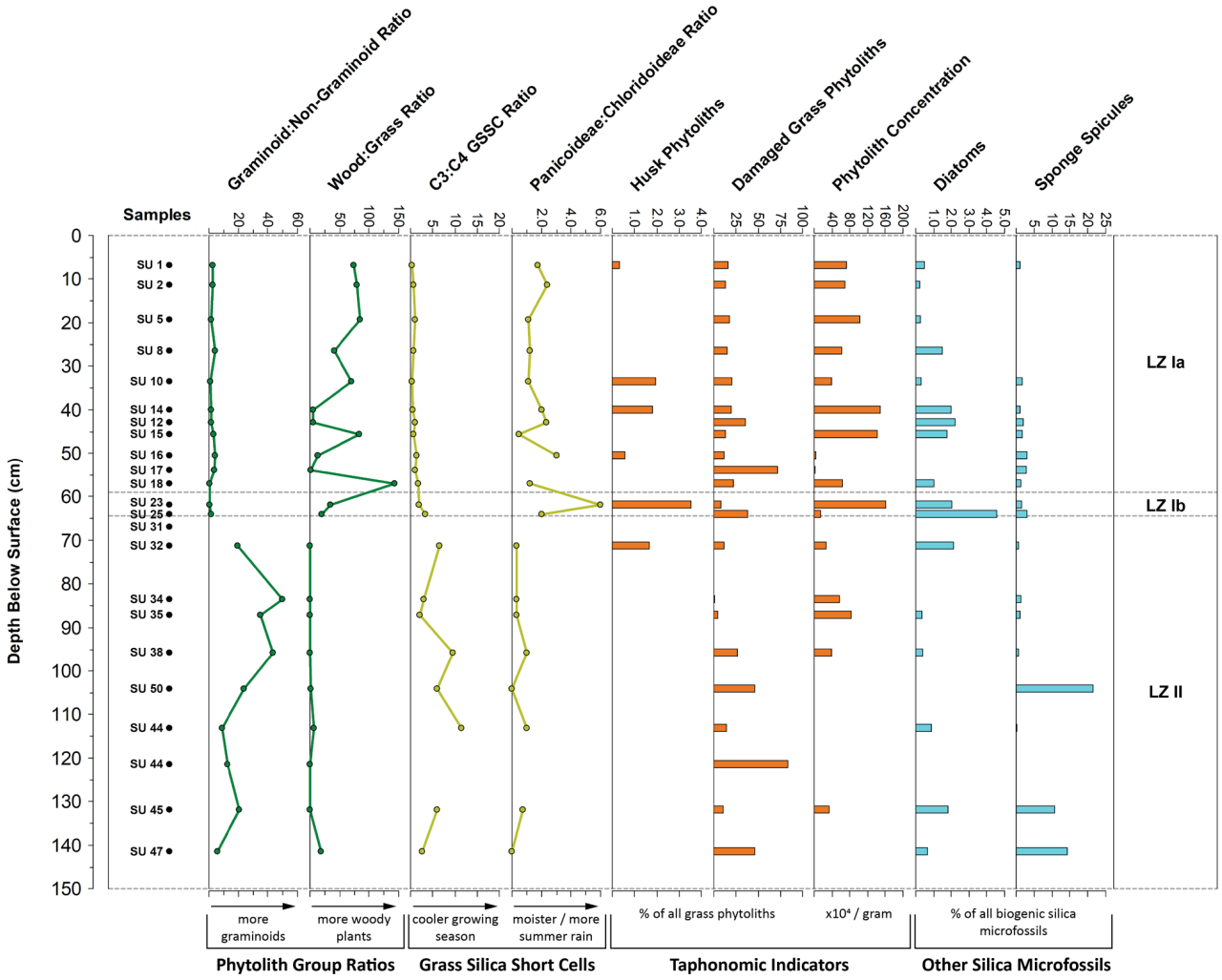

Figure 7: Stratigraphic presentation of phytolith ratios and taphonomic indicators, as well as the proportions of recovered diatoms and sponge spicules. Figure produced by Christopher Ames.

enough diagnostic short cells to be included in the Panicoideae to Chloridoideae ratio. In LZ II, SU 31 did not produce any biogenic silica microfossils, and the lower sample from SU 44 did not produce enough diagnostic short cells to be included in the GSSC ratios (Supplementary file 3).

In the recovered samples from LZ II, graminoids dominate the signal and C_3 types dominate the grass phytoliths—C_3 to C_4 ratios are in the range of 6:1 and reaching as high as 16:1 (**Figure 7**). Of the identifiable C_4 grasses, the drought-resistant Chloridoideae are slightly more abundant with Panicoideae to Chloridoideae ratios at or below one. Diatoms are present in low levels throughout, whereas sponge spicules are more abundant in the lower SUs of LZ II, and relatively sparse toward the upper boundary. Husk phytoliths appear in the uppermost part of LZ II, which coincides with increased charcoal and artefact concentrations in the coarse fraction.

Phytoliths are relatively well preserved in LZ Ib and have slightly lower rates of damage than the underlying zone. Graminoids are close to even in abundance with non-graminoids, having ratios of 1.3 and 0.80 for SU 25 and 23 respectively. Woody plants—indicated by the presence of spherical phytoliths—are more common than in LZ II. C_3 types are most abundant in the identifiable grasses, although significantly less so than in LZ II, with C_3 to C_4 ratios of 3:1 and 1:1. Of the C_4 grasses, the mesic Panicoideae are most abundant as the Panicoideae to Chloridoideae ratio is 2.0 for SU 25 and 6.0 for SU 23. Zone Ib has the highest proportion of husk phytoliths and diatoms for the entire sequence, with a small proportion of sponge spicules present as well.

Phytolith concentrations remain relatively high in LZ Ia, with the exception of samples from SU 16 and 17. Despite some of the lowest rates of damaged phytoliths in the entire sequence, damaged phytolith proportions are still in the range of 12–35% (excluding SU 17 that has 73% damaged phytoliths). Other than for SU 18, graminoids are more abundant than non-graminoids with ratios between 1.2 and 4.4. Woody plants are considerably more abundant than grasses, although the ratio varies significantly between 1.0 and 144.0. Within the grasses, the C_3 to C_4 ratio declines from the bottom to the top of the sequence. The bottom five samples have a slight abundance of C_3 type grasses (ratios from 0.7–1.7) whereas the top six samples have a slight abundance of C_4 type grasses (ratios from 0.4–1.0). Within the C_4 grasses assemblage, the mesic Panicoideae are more abundant than the drought-resistant Chloridoideae, with ratios of 1.1–3.0 except for SU 15 that has a ratio of 0.5. Husk phytoliths occur sporadically through LZ Ia (SUs 1, 10, 14, and 16), and diatoms and sponge spicules are present in low quantities in most samples.

6. Discussion

6.1. Site formation and palaeoenvironmental context

Zone II accumulated relatively slowly during Marine Isotope Stage (MIS) 3 with frequent, potentially intermittent human occupations, indicated by relatively low artefact and charcoal abundances and the relatively small lenses and isolated thin layers of charcoal-rich sediment. Based on the artefact densities recorded during the 1979 excavation, this pattern of occupation and accumulation was reasonably consistent throughout LZ II, although there is an increase in occupational intensity markers from bulk sediments immediately prior to the carbonate crust development capping this LZ.

Given the evidence for combustion features throughout LZ II, the lack of phytoliths from woody plants and the almost non-existent calcite signal is suspicious. The burning that produced the charcoal would have also produced ash (i.e., calcite), and if wood was being used as fuel we would expect these phytoliths to be present, even if in small quantities. The baseline presence of sponge spicules with notable spikes of higher concentration indicates moist sedimentary conditions. This, plus the clay coatings lining pore spaces observed in the ongoing microstratigraphic analysis, indicate gentle post-depositional water movement through the profile possibly dissolving the ash in addition to translocating clays (Christopher Ames, unpublished data). Such dissolution is also likely to have affected bone preservation in these layers, for which recovery rates are significantly lower (Collins, Wilkins & Ames 2017; Opperman 1987). Wood phytoliths, moreover, are non-existent in all but three samples from LZ II. High alkalinity and water flow can degrade phytoliths (Piperno 2006), and this may be contributing to reduced phytolith preservation in LZ II. However, there are plenty of recovered grass phytoliths so the absence of phytoliths from woody plants is likely not a preservation issue, suggesting that woody plants were not the primary fuel source, but rather grasses and sedges (i.e., graminoids) were burned during the MIS 3 occupations. Although it is possible this represents selective fuel harvesting, many woody plants inhabit the current landscape in front of Grassridge (see **Figure 2**), and it seems most parsimonious that fewer woody plants were available in the Stormberg grasslands during MIS 3. This interpretation is supported by the C_3 dominated grasslands and the presence of drought-resistant C_4 morphotypes, which indicate cooler and drier conditions respectively at this time. However, the presence of C_4 grasses also indicates that although conditions were overall drier, there was at least some year round rainfall during the MIS 3 occupations at Grassridge. Detailed examination of fuel use is also part of the active microstratigraphic analysis.

The carbonate crust development at the top of LZ II is anomalous, as calcium carbonate is relatively rare across the sandstone-dominated landscape. The carbonate crust has an undulating surface and is thinner toward the back of the shelter (~1 cm), becoming thicker (1–3 cm) with weakly expressed laminations toward the dripline. This structure combined with the implied landscape stability of LZ II-Ib boundary from the higher levels of iron-bearing minerals, suggest the crust is the remnant of a microbial mat, which was lithified into calcium carbonate (Chafetz & Buczynski 1992; Freytet & Verrecchia 1995; Riding 2000; Northup & Lavoie 2001; Morley et al. 2017). The spike in diatom concentration immediately above the boundary implies it may have been an algal mat blanketing parts of the rock shelter floor. Additional work is ongoing

regarding the characterisation and formation of the crust as part of the microstratigraphic analysis, but similar mats currently grow in patches at the back of the rock shelter where water seeps in and saturates isolated parts of the surface. Coinciding with the interpretation of the crust as a stable, surface-covering microbial mat is the long period of time this 1–3 cm represents in the stratigraphic sequence. Based on median ages, the carbonate crust and overlying unconformity encompass 28.1–13.5 ka, aligning very closely with MIS 2 (29–14 ka). Moreover, a microbial mat covering much of the rock shelter floor suggests there was some water seeping into the rock shelter during at least the early parts of MIS 2, and provides a mechanism for the translocation of fine particles and the dissolution ash in LZ II. Moreover, once this crust was sufficiently developed, the resulting hardened surface could promote runoff and the erosion of accumulating sediments (Morley et al. 2017), which may explain the gap in deposition between LZ II and Ib. However, it is currently unclear how much of MIS 2 relates to the microbial mat and crust formation and how much is represented by the overlying unconformity.

Following the roughly 15 kyr depositional gap at Grassridge, human occupation and sediment deposition return concurrently at approximately 13.5 ka, nearly coincident with the start of MIS 1 (14 ka–Present). Zone Ib is thin and represents approximately 2 kyr, accumulating during most of the Younger Dryas (i.e., 13–11.5 ka) at a similar rate to the MIS 3 deposits. The large diameter combustion feature and high artefact abundance in this LZ point to high intensity use of the shelter at this time. The phytolith ratios indicate the environment was more similar to modern conditions—predominantly grassland with some woody vegetation. The latter were likely brought into the shelter as fuel. The relatively even proportions of C_3 and C_4 grasses point to somewhat cooler growing conditions than today, whereas the predominance of Panicoideae indicates overall slightly moister conditions, with a likely increase in summer rainfall compared to LZ II, a combination that suggests some year round rainfall in the area around Grassridge during the Younger Dryas.

Zone Ib ends abruptly at 11.6 ka and is followed by a 4–5 kyr gap in deposition before occupation begins again about 7.3 ka. There is broad correlation for the end of the Younger Dryas event at this time in South Africa (Stewart & Mitchell 2018; Truc et al. 2013). However, caution is required here because the abrupt sedimentary transition between LZ Ib and Ia indicates that the latter truncates the former. As such, an unknown amount of sediment has been removed from the top of LZ Ib, perhaps by erosion or as part of hearth construction by the mid-Holocene inhabitants. It is thus likely that some early Holocene occupation has been removed; how much is presently unclear. Although this question cannot be answered with the small areal coverage of the current excavations, we can be certain that if an occupational gap does exist in the early Holocene record at Grassridge, it was shorter than recorded in our chrono-stratigraphic results and thus may not be associated with the end of the Younger Dryas. Only expanding sub-surface exploration in the shelter will help resolve this uncertainty around the LZ Ib-Ia boundary.

LZ Ia accumulated rapidly in the mid-Holocene during a 500–600 year period of intense occupation between 7.3–6.8 ka. The entire sedimentary sequence is indicative of hearth construction and reuse. There are intact combustion features with the characteristic triplets of stratified ash, charcoal, and rubefied sediment (Goldberg & Bar-Yosef 2002; Meignen et al. 2007), interdigitated with thick layers of ashy sediments with disaggregated and randomly distributed combustion feature components indicative of hearth rake out and dumping (Goldberg et al. 2009; Miller et al. 2009). An interpretation of hearth construction and maintenance is supported by the extremely high quantities of woody plant phytoliths from these layers, as well as vast quantities of burnt and calcined bone recovered from LZ Ia during the renewed and ongoing excavations (Collins, Wilkins & Ames 2017). The GSSCs document an environment transitioning from a slightly cooler growing season to conditions more similar to modern day, dominated by warm temperatures and summer rainfall with dry winters.

6.2. Late Quaternary occupation in the high altitude grasslands

The oldest occupation zone at Grassridge (43–28 ka) is associated with plain platform, flake dominated MSA archaeology with very few retouched implements and points (Opperman 1988). As such, the stone tools from LZ II are broadly consistent with other late and final MSA assemblages from MIS 3 documented in southern Africa (Lombard et al. 2012). Relative to the Holocene layers, the MIS 3 occupation sequence is low intensity. Yet, stone artefacts are common throughout and there are scattered combustion features indicating at least semi-continuous habitation over this 15 kyr in a cooler, drier grassland environment than seen in the region today. Moreover, with similarly aged occupation horizons identified at Rose Cottage Cave (Wadley 2004, 1997), Ha Makotoko (Mitchell & Arthur 2014), Strathalan B (Opperman 1996; Opperman & Heydenrych 1990), Sehonghong (Mitchell 1994; Pargeter, Loftus & Mitchell 2017), Melikane (Stewart et al. 2012), and likely at Highlands rock shelter (Deacon 1976) and Ntloana Tšoana (Jacobs et al. 2008; Mitchell & Steinberg 1992), MIS 3 appears to have been a period of relatively widespread human habitation across different biogeoclimatic zones in the interior of southern Africa. However, more detailed assessment of the technological and subsistence strategies practised by the MIS 3 inhabitants at Grassridge—and how they relate to nearby interior grassland, montane, near-coastal, and coastal sites—must await completion of the ongoing analysis of the newly excavated material.

Regional records suggest a cold, dry environment during MIS 2 (Lewis 2008), which might partially explain the occupational gap at this time at Grassridge. However, the remnants of the microbial mat indicate that some water was readily available at the termination of MIS 3 and possibly a portion of MIS 2 at Grassridge. Occupation of the Sub-Escarpment Grassland bioregion during the early part of MIS 2 is documented at Strathalan B (Opperman 1996, 1992), where the uppermost archaeological remains date

no younger than 23.9–22.3k cal a BP at the 95.4% confidence level (Pta-4944: 20 900 ± 350 ^{14}C a BP; calibrated using same method as outlined above; age reported in Opperman & Heydenrych 1990). Sehonghong and Rose Cottage Cave were also occupied in the early part of MIS 2 (Mitchell 1996; Pargeter, Loftus & Mitchell 2017; Wadley 1997), both at higher altitude. Currently, the only known occupations dating to the latter portion of MIS 2 (19–14 ka) are Robberg-like from Rose Cottage Cave (Wadley 1996, 1995), Ha Makotoko (Mitchell & Arthur 2014), and perhaps ephemerally at Sehonghong (Mitchell 1995; Pargeter, Loftus & Mitchell 2017), again all at higher altitude. With relatively few data points overall from MIS 2, and particularly for the 19–14 ka window, it is difficult to make broad statements regarding settlement patterns during the LGM. As both Robberg-like and final MSA-like flake-blade assemblages are associated with the MIS 2 sites (Clark 1997; Mitchell 1995), it seems to have been a period of increased technological variation—possibly as foragers adapted differentially to environmental reorganisation during the LGM. Moreover, the data that does exist is concentrated in the montane regions, leading some to suggest the colder and drier conditions in the latter part of MIS 2 (Scott et al. 2012) ultimately resulted in population contraction around more reliable freshwater sources at the higher altitudes of the Maloti-Drakensberg (Pargeter et al. 2017; Stewart & Mitchell 2018). This is a hypothesis that warrants continued evaluation within the Grassland and Mesic Highveld bioregions of the Maloti-Drakensberg and, importantly, in the slightly lower elevation surrounding regions.

The terminal Pleistocene occupation at Grassridge is associated with the Later Stone Age artefact types from layer LBS in the 1979 sequence, such as large end and side scrapers (Collins, Wilkins & Ames 2017; Opperman 1988, 1984), and cooler and moister grassland conditions with woody vegetation likely growing along stream margins. Although Opperman did not identify a terminal Pleistocene layer, he did observe that hornfels was more common in LBS than in the overlying layers, and considered his observed change in scraper morphology from bottom (LBS, AS) to top (HSK, BR, VB) to be consistent with a transition from early Holocene types to mid Holocene types. Based on our chrono-stratigraphic result, LBS is predominantly terminal Pleistocene in age, with the larger scrapers and lack of backed segments suggesting a more Oakhurst-like assemblage (Collins, Wilkins & Ames 2017; Lombard et al. 2012). We must also bear in mind that there is likely some mixing of MIS 3, terminal Pleistocene, and mid-Holocene artefacts in Opperman's summaries, as LBS appears to encompass deposits immediately above and below the carbonate crust, as well as some of the basal deposits of LZ Ia. Opperman's acknowledgment that there appeared to be some mixing across the MSA-LSA boundary in his sequence supports this notion (Opperman 1988). More detailed examination of the archived stone tool assemblage is planned alongside finalising the analysis of the newly excavated material. We can currently report that, at least chronologically, the terminal Pleistocene Oakhurst-like occupation at Grassridge overlaps with similar assemblages from Ha Makotoko (Mitchell & Arthur 2014) and Te Vrede (Opperman 1987), and Robberg-like assemblages from Sehonghong (Mitchell 1996; Pargeter, Loftus & Mitchell 2017) and Ravenscraig (Opperman 1987). However, it is slightly older than the Oakhurst assemblage from Rose Cottage Cave (Wadley 2000a, 1997).

The brief and very intense mid-Holocene occupation, bracketed between 7.3–6.8 ka, contains Wilton artefact types, including relatively small end scrapers and backed segments (Collins, Wilkins & Ames 2017; Opperman 1987). The mid-Holocene was warm and with moisture much more concentrated in summer. The studied sequence provides no evidence for occupation younger than 6.8 ka. Mid-Holocene occupation at Grassridge coincides with expansion and intensification of Wilton occupation at other sites in the high elevation grasslands, such as Rose Cottage Cave (Wadley 2000b), Sehonghong (Mitchell & Vogel 1994), and Tloutle (Mitchell 1990), as well as at sites in the Fish River basin to the southwest (Hall 2000; Lewis 2002). Importantly, the nature of the mid-Holocene sediments indicates that during this time the southwest portion of the shelter was the focus of intensive, repetitive hearth construction. The mounded ashy sediments here are an obvious topographic feature within the shelter. Considering we believe this period of hearth construction scoured away some of the terminal Pleistocene deposit, we should be cautious in interpreting the studied profile as fully representative of the MIS 1 habitation sequence, and something that may possibly be contributing to the pulsed signal at other sites in the region. This is particularly relevant when considering the multiple episodes of rock paintings in and around Grassridge and the isolated ceramic sherds located in the artefact-rich palimpsests in front of the shelter (Collins, Wilkins & Ames 2017). Not to mention that the combined 1979 and renewed GAPP excavations (9 m^2) only represent a tiny portion of the shelter surface area (>225 m^2). As demonstrated by excavations at Ha Makotoko (Mitchell & Arthur 2014), spatially varying rates of sediment accumulation and differential preservation can create significant differences in the chrono-stratigraphic sequence throughout large rock shelters.

7. Conclusion

Sedimentation is highly variable throughout the Grassridge stratigraphic sequence and is likely driven by human presence, with three occupational pulses identified at 43–28 ka, 13.5–11.6 ka, and 7.3–6.8 ka. Each occupational pulse is associated with a different stone tool technocomplex for which analyses of recently excavated material are in progress. Recovered phytolith assemblages document a transition from cooler, C_3 dominated grasslands and more year round rainfall in the latter part of MIS 3 to a warmer, C_4 dominated grassland in the mid-Holocene—the latter indicative of an environment similar to that observed today. In between these two endpoints, during the Younger Dryas, the equal proportions of C_3 and C_4 grasses indicate cooler overall

conditions, likely with a predominance of rainfall in the summer months. The two distinct depositional and occupational breaks in the stratigraphic sequence occur during MIS 2 (28–14 ka) and the early Holocene (11.6–7.3 ka)—the latter ages potentially misleading due to the truncation of older sediments by more recent episodes of hearth construction.

The revised chrono-stratigraphic sequence confirms the continuation of MSA technology at sites in the interior of South Africa until the end of MIS 3, and places Grassridge as one of very few interior sites that preserve occupation from the Younger Dryas. Expanded excavation is required at Grassridge to determine if this occupational sequence is a site-wide phenomenon. However, the pulsed occupational sequence identified is characteristic of the Pleistocene and Holocene record across the greater region. Based on currently available evidence, which is limited for the Late Pleistocene, this pattern seems linked to a complex system of mobility entwined with rapidly fluctuating palaeoenvironments across a period characterised by high palaeoclimatic variability. Only with continued research can this model be tested and the nature of interaction between inhabitants of the highland grasslands and those in the somewhat more intensively studied Maloti-Drakensberg region (Stewart & Mitchell 2018), as well as with the emerging record from the Pondoland coast (Fisher et al. 2013) be established.

Additional Files

The additional files for this article can be found as follows:

- **Supplementary file 1.** Optically Stimulated Luminescence Methodological and Results Detail. DOI: https://doi.org/10.5334/oq.77.s1
- **Supplementary file 2.** Stratigraphic and Sedimentological Field Observations and Laboratory Data. DOI: https://doi.org/10.5334/oq.77.s2
- **Supplementary file 3.** Biogenic Silica Microfossil Methodological and Results Detail. DOI: https://doi.org/10.5334/oq.77.s3

Acknowledgements

We would like to thank Dr Hermanus Opperman for sharing his insights with us regarding the original 1979 excavations, as well as Constance Neyabo, Sylvia Mazixana, Andreas Leroux, Cherene DeBruyn, Lisa Rogers, Ayanda Mdludlu, and Catherine van Oort for their participation in the excavation and analyses of materials from 2014–2019. We are indebted to Jill and the late Roy Callaghan who allowed us to work on their land and provided an unprecedented level of hospitality during our field research. For permissions and research support, we thank the Eastern Cape Heritage Resources Authority (Excavation permit: 2/2/APM-PERMIT/14/05/001), The Albany Museum, The South African Heritage Resources Authority, and the Department of Archaeology at the University of Cape Town. We also thank Peter Mitchell and one anonymous reviewer for their feedback on an earlier version of this manuscript.

Funding Information

The Grassridge Archaeological and Palaeoenvironmental Project has received funding from The Leakey Foundation, The Wenner-Gren Foundation (Post PhD Grant #9144), and the Social Sciences and Humanities Research Council of Canada (Insight Development Grant #430-2017-965) to support various components of the research presented in this manuscript.

Competing Interests

The authors have no competing interests to declare.

Author Contributions

CA and BC conceptualised this study, with significant contributions to data acquisition and interpretation by CA, LG, CC, KB, BJ, LM, and BC. CA primarily drafted the manuscript with critical input and revision from all other authors.

References

Aarnes, I, Svensen, H, Polteau, S and **Planke, S.** 2011. Contact metamorphic devolatilization of shales in the Karoo Basin, South Africa, and the effects of multiple sill intrusions. *Chemical Geology*, 281: 181–194. DOI: https://doi.org/10.1016/j.chemgeo.2010.12.007

Barham, L and **Mitchell, P.** 2008. *The first Africans: African archaeology from the earliest tool makers to most recent foragers*. Cambridge: Cambridge University Press. DOI: https://doi.org/10.1017/CBO9780511817830

Bordy, EM and **Catuneanu, O.** 2002. Sedimentology of the Beaufort-Molteno Karoo fluvial strata in the Tuli Basin, South Africa. *South African Journal of Geology*, 105: 51–66. DOI: https://doi.org/10.2113/1050051

Bordy, EM and **Eriksson, P.** 2015. Lithostratigraphy of the Elliot Formation (Karoo Supergroup), South Africa. *South African Journal of Geology*, 118: 311–316. DOI: https://doi.org/10.2113/gssajg.118.3.311

Bronk Ramsey, CB and **Lee, S.** 2013. Recent and Planned Developments of the Program Oxcal. *Radiocarbon*, 55: 720–730. DOI: https://doi.org/10.2458/azu_js_rc.55.16215

Castro, DJ and **Bell, FG.** 1995. An engineering geological appraisal of the sandstones of the Clarens Formation, Lesotho, in relation to tunnelling. *Geotechnical & Geological Engineering*, 13: 117–142. DOI: https://doi.org/10.1007/BF00456713

Chafetz, HS and **Buczynski, C.** 1992. Bacterially Induced Lithification of Microbial Mats. *PALAIOS*, 7: 277–293. DOI: https://doi.org/10.2307/3514973

Chazan, M. 2015. Technological Trends in the Acheulean of Wonderwerk Cave, South Africa. *African Archaeological Review*, 32: 701–728. DOI: https://doi.org/10.1007/s10437-015-9205-8

Chazan, M, Ron, H, Matmon, A, Porat, N, Goldberg, P, Yates, R, Avery, M, Sumner, A and **Horwitz,**

LK. 2008. Radiometric dating of the Earlier Stone Age sequence in Excavation I at Wonderwerk Cave, South Africa: preliminary results. *Journal of Human Evolution*, 55: 1–11. DOI: https://doi.org/10.1016/j.jhevol.2008.01.004

Chevallier, L and **Woodford, A.** 1999. Morpho-tectonics and mechanism of emplacement of the dolerite rings and sills of the western Karoo, South Africa. *South African Journal of Geology*, 102: 43–53.

Clark, AMB. 1997. The final Middle Stone Age at Rose Cottage Cave: a distinct industry in the Basutolian ecozone. *South African Journal of Science*, 93: 449–458.

Coetzee, A and **Kisters, A.** 2016. The 3D geometry of regional-scale dolerite saucer complexes and their feeders in the Secunda Complex, Karoo Basin. *Journal of Volcanology and Geothermal Research*, 317: 66–79. DOI: https://doi.org/10.1016/j.jvolgeores.2016.04.001

Collins, BR, Wilkins, J and **Ames, CJH.** 2017. Revisiting the Holocene Occupations at Grassridge Rockshelter, Eastern Cape, South Africa. *The South African Archaeological Bulletin*, 72: 162–170.

Deacon, HJ. 1976. *Where hunters gathered: a study of Holocene Stone Age people in the eastern Cape*. Claremont, South Africa: South African Archaeological Society.

Dean, WE. 1974. Determination of carbonate and organic matter in calcareous sediments and sedimentary rocks by loss on ignition; comparison with other methods. *Journal of Sedimentary Research*, 44: 242–248. DOI: https://doi.org/10.1306/74D729D2-2B21-11D7-8648000102C1865D

Ecker, M, Brink, J, Chazan, M, Horwitz, LK and **Lee-Thorp, JA.** 2017. Radiocarbon Dates Constrain the Timing of Environmental and Cultural Shifts in the Holocene Strata of Wonderwerk Cave, South Africa. *Radiocarbon*, 59: 1067–1086. DOI: https://doi.org/10.1017/RDC.2017.55

Fisher, EC, Albert, RM, Botha, G, Cawthra, HC, Esteban, I, Harris, J, Jacobs, Z, Jerardino, A, Marean, CW, Neumann, FN, Pargeter, J, Poupart, M and **Venter, J.** 2013. Archaeological Reconnaissance for Middle Stone Age Sites Along the Pondoland Coast, South Africa. *PaleoAnthropology*, 2013: 104–137.

Freytet, P and **Verrecchia, E.** 1995. Discovery of Ca oxalate crystals associated with fungi in moss travertines (bryoherms, freshwater heterogeneous stromatolites). *Geomicrobiology Journal*, 13: 117–127. DOI: https://doi.org/10.1080/01490459509378010

Galbraith, RF, Roberts, RG, Laslett, GM, Yoshida, H, and **Olley, JM.** 1999. Optical Dating of Single and Multiple Grains of Quartz from Jinmium Rock Shelter, Northern Australia: Part I, Experimental Design and Statistical Models. *Archaeometry*, 41: 339–364. DOI: https://doi.org/10.1111/j.1475-4754.1999.tb00987.x

Gliganic, LA, Cohen, TJ, Meyer, M and **Molenaar, A.** 2017. Variations in luminescence properties of quartz and feldspar from modern fluvial sediments in three rivers. *Quaternary Geochronology*, 41: 70–82. DOI: https://doi.org/10.1016/j.quageo.2017.06.005

Gliganic, LA, May, J-H and **Cohen, TJ.** 2015. All mixed up: Using single-grain equivalent dose distributions to identify phases of pedogenic mixing on a dryland alluvial fan. *Quaternary International*, 362: 23–33. DOI: https://doi.org/10.1016/j.quaint.2014.07.040

Goldberg, P and **Bar-Yosef, O.** 2002. Site formation processes in Kebara and Hayonim Caves and their significance in Levantine prehistoric caves. In: Akazawa, T, Aoki, K and Bar-Yosef, O (eds.), *Neandertals and modern humans in Western Asia*, 107–125. New York: Plenum Press. DOI: https://doi.org/10.1007/0-306-47153-1_8

Goldberg, P, Miller, CE, Schiegl, S, Ligouis, B, Berna, F, Conard, NJ and **Wadley, L.** 2009. Bedding, hearths, and site maintenance in the Middle Stone age of Sibudu cave, KwaZulu-Natal, South Africa. *Archaeological and Anthropological Sciences*, 1: 95–122. DOI: https://doi.org/10.1007/s12520-009-0008-1

Grab, S. 2015. Sandstone Landforms of the Karoo Basin: Naturally Sculpted Rock. In: Grab, S and Knight, J (eds.), *Landscapes and Landforms of South Africa*, 11–21. Springer International Publishing. DOI: https://doi.org/10.1007/978-3-319-03560-4_2

Hall, S. 2000. Burial and Sequence in the Later Stone Age of the Eastern Cape Province, South Africa. *The South African Archaeological Bulletin*, 55: 137–146. DOI: https://doi.org/10.2307/3888962

Hallinan, E and **Parkington, J.** 2017. Stone Age landscape use in the Olifants River Valley, Clanwilliam, Western Cape, South Africa. *Azania: Archaeological Research in Africa*, 52: 324–372. DOI: https://doi.org/10.1080/0067270X.2017.1365438

Heiri, O, Lotter, AF and **Lemcke, G.** 2001. Loss on ignition as a method for estimating organic and carbonate content in sediments: reproducibility and comparability of results. *Journal of Paleolimnology*, 25: 101–110. DOI: https://doi.org/10.1023/A:1008119611481

Hendershot, WH, Lalande, H and **Duquette, M.** 1993. Soil Reaction and Exchangeable Acidity. In: Carter, MR (ed.), *Soil sampling and methods of analysis*, 141–145. Boca Raton, USA: Lewis Publishers.

Hoare, DB and **Bredenkamp, GJ.** 2001. Syntaxonomy and environmental gradients of the grasslands of the Stormberg/Drakensberg mountain region of the Eastern Cape, South Africa. *South African Journal of Botany*, 67: 595–608. DOI: https://doi.org/10.1016/S0254-6299(15)31189-3

Hogg, AG, Hua, Q, Blackwell, PG, Niu, M, Buck, CE, Guilderson, TP, Heaton, TJ, Palmer, JG, Reimer, PJ, Reimer, RW, Turney, CSM and **Zimmerman, SRH.** 2013. SHCal13 Southern Hemisphere Calibration, 0–50,000 Years cal BP. *Radiocarbon*, 55: 1889–1903. DOI: https://doi.org/10.2458/azu_js_rc.55.16783

Jacobs, Z, Roberts, RG, Galbraith, RF, Deacon, HJ, Grün, R, Mackay, A, Mitchell, P, Vogelsang, R and **Wadley, L.** 2008. Ages for the Middle Stone Age of southern Africa: Implications for human behavior and dispersal. *Science*, 322: 733–735. DOI: https://doi.org/10.1126/science.1162219

Joines, JP. 2011. 17,000 Years of Climate Change: The Phytolith Record from Hall's Cave, Texas. Unpublished thesis (Msc), Oklahoma State University. Available at URL https://shareok.org/handle/11244/9038 [last accessed 5 August 2019].

Juggins, S. 2014. *C2 Home, C2 Version 1.7.7*. Available at URL https://www.staff.ncl.ac.uk/stephen.juggins/software/C2Home.htm [last accessed 6 August 2019].

Kitching, JW and **Raath, MA.** 1984. Fossils from the Elliot and Clarens Formations (Karoo sequence) of the Northeastern Cape, Orange Free State and Lesotho, and a suggested biozonation based on tetrapods. *Palaeontologica Africana*, 25: 111–125.

Kuman, K, Sutton, MB, Pickering, TR and **Heaton, JL.** 2018. The Oldowan industry from Swartkrans cave, South Africa, and its relevance for the African Oldowan. *Journal of Human Evolution*, 123: 52–69. DOI: https://doi.org/10.1016/j.jhevol.2018.06.004

Lentfer, CJ and **Boyd, WE.** 1998. A Comparison of Three Methods for the Extraction of Phytoliths from Sediments. *Journal of Archaeological Science*, 25: 1159–1183. DOI: https://doi.org/10.1006/jasc.1998.0286

Lewis, CA. 2002. Radiocarbon dates and the Late Quaternary palaeogeography of the Province of the Eastern Cape, South Africa. *Quaternary International*, 89: 59–69. DOI: https://doi.org/10.1016/S1040-6182(01)00081-7

Lewis, CA. 2008. Late Quaternary climatic changes, and associated human responses, during the last ~45000 yr in the Eastern and adjoining Western Cape, South Africa. *Earth-Science Reviews*, 88: 167–187. DOI: https://doi.org/10.1016/j.earscirev.2008.01.006

Lin, SC, Douglass, MJ and **Mackay, A.** 2016. Interpreting MIS3 artefact transport patterns in Southern Africa using cortex ratios: An example from the putslaagte valley, Western Cape. *The South African Archaeological Bulletin*, 71: 173–180.

Lombard, M, Wadley, L, Deacon, J, Wurz, S, Parsons, I, Mohapi, M, Swart, J and **Mitchell, P.** 2012. South African and Lesotho Stone Age Sequence Updated. *The South African Archaeological Bulletin*, 67: 123–144.

Lukich, V, Porat, N, Faershtein, G, Cowling, S and **Chazan, M.** 2019. New Chronology and Stratigraphy for Kathu Pan 6, South Africa. *Journal of Paleolithic Archaeology*, 2: 235–257. DOI: https://doi.org/10.1007/s41982-019-00031-7

Mackay, A, Sumner, A, Jacobs, Z, Marwick, B, Bluff, K and **Shaw, M.** 2014. Putslaagte 1 (PL1), the Doring River, and the later Middle Stone Age in southern Africa's Winter Rainfall Zone. *Quaternary International*, 350: 43–58. DOI: https://doi.org/10.1016/j.quaint.2014.05.007

Marean, CW. 2014. The origins and significance of coastal resource use in Africa and Western Eurasia. *Journal of Human Evolution*, 77: 17–40. DOI: https://doi.org/10.1016/j.jhevol.2014.02.025

Marean, CW. 2016. The transition to foraging for dense and predictable resources and its impact on the evolution of modern humans. *Philosophical Transactions of the Royal Society B: Biological Sciences*, 371: 20150239. DOI: https://doi.org/10.1098/rstb.2015.0239

Meignen, L, Goldberg, P and **Bar-Yosef, O.** 2007. The Hearths at Kebara Cave and their Role in Site Formation Processes. In: Bar-Yosef, O and Meignen, L (eds.), *Kebara Cave, Mt Carmel, Israel: The Middle and Upper Paleolithic Archaeology, Part I*, 91–122. Cambridge, USA: Harvard University Press.

Miller, CE, Conard, NJ, Goldberg, P and **Berna, F.** 2009. Dumping, sweeping and trampling: experimental micromorphological analysis of anthropogenically modified combustion features. In: Théry-Parisot, I, Chabal, L and Costamagno, S (eds.). *The taphonomy of Burned Organic Residues and Combustion Features in Archaeological Contexts, Proceedings of the round table*, May 27–29 2008, CEPAM, P@lethnology, 2, 25–37.

Miller, CE, Goldberg, P and **Berna, F.** 2013. Geoarchaeological investigations at Diepkloof Rock Shelter, Western Cape, South Africa. *Journal of Archaeological Science*, 40: 3432–3452. DOI: https://doi.org/10.1016/j.jas.2013.02.014

Mitchell, P and **Arthur, C.** 2014. Ha Makotoko: Later Stone Age Occupation across the Pleistocene/Holocene Transition in Western Lesotho. *Journal of African Archaeology*, 12: 205–232. DOI: https://doi.org/10.3213/2191-5784-10255

Mitchell, PJ. 1990. Preliminary Report on the Later Stone Age Sequence from Tloutle Rock Shelter, Western Lesotho. *The South African Archaeological Bulletin*, 45: 100–105. DOI: https://doi.org/10.2307/3887968

Mitchell, PJ. 1994. Understanding the MSA/LSA transition: the pre-20 000 BP assemblages from new excavations at Sehonghong:rock shelter, Lesotho. *Southern African Field Archaeology*, 3: 15–25.

Mitchell, PJ. 1995. Revisiting the Robberg: New Results and a Revision of Old Ideas at Sehonghong Rock Shelter, Lesotho. *The South African Archaeological Bulletin*, 50: 28–38. DOI: https://doi.org/10.2307/3889272

Mitchell, PJ. 1996. The late Quaternary of the Lesotho highlands, southern Africa: Preliminary results and future potential of ongoing research at Sehonghong shelter. *Quaternary International*, 33: 35–43. DOI: https://doi.org/10.1016/1040-6182(95)00097-6

Mitchell, PJ and **Steinberg, JM.** 1992. Ntloana Tsoana: A Middle Stone Age Sequence from Western Lesotho. *The South African Archaeological Bulletin*, 47: 26–33. DOI: https://doi.org/10.2307/3888989

Mitchell, PJ and **Vogel, JC.** 1994. New radiocarbon dates from Sehonghong Rock Shelter, Lesotho. *South African Journal of Science*, 90: 284–288.

Morley, MW, Goldberg, P, Sutikna, T, Tocheri, MW, Prinsloo, LC, Jatmiko, Saptomo, EW, Wasisto, S and **Roberts, RG.** 2017. Initial micromorphological results from Liang Bua, Flores (Indonesia): Site formation processes and hominin activities at the type locality of Homo floresiensis. *Journal of Archaeological Science*, 77: 125–142. DOI: https://doi.org/10.1016/j.jas.2016.06.004

Mucina, L and **Rutherford, MC.** 2006. *The vegetation of South Africa, Lesotho and Swaziland*. Pretoria: South African National Biodiversity Institute.

Murray, AS and **Wintle, AG.** 2000. Luminescence dating of quartz using an improved single-aliquot regenerative-dose protocol. *Radiation Measurements*, 32: 57–73. DOI: https://doi.org/10.1016/S1350-4487(99)00253-X

Northup, DE and **Lavoie, KH.** 2001. Geomicrobiology of Caves: A Review. *Geomicrobiology Journal*, 18: 199–222. DOI: https://doi.org/10.1080/01490450152467750

Opperman, H. 1984. A report on Excavations at Grassridge Rock Shelter, Sterkstroom District, Cape Province. *Fort Hare Papers*, 7: 391–406.

Opperman, H. 1987. *The later stone age of the Drakensberg Range and its foothills*. Oxford: BAR Publishing.

Opperman, H. 1988. An excavation of a Middle Stone Age deposit in Grassridge Rockshelter, Sterkstroom District, Cape Province. *Fort Hare Papers*, 9: 51–61.

Opperman, H. 1992. A report on the results of a test pit in Strathalan Cave B, Maclear district, North-eastern Cape. *Southern African Field Archaeology*, 1: 98–102.

Opperman, H. 1996. Strathalan Cave B, north-eastern Cape Province, south Africa: Evidence for human behaviour 29,000–26,000 years ago. *Quaternary International*, 33: 45–53. DOI: https://doi.org/10.1016/1040-6182(95)00096-8

Opperman, H and **Heydenrych, B.** 1990. A 22 000 Year-Old Middle Stone Age Camp Site with Plant Food Remains from the North-Eastern Cape. *The South African Archaeological Bulletin*, 45: 93–99. DOI: https://doi.org/10.2307/3887967

Pargeter, J, Loftus, E and **Mitchell, P.** 2017. New ages from Sehonghong rock shelter: Implications for the late Pleistocene occupation of highland Lesotho. *Journal of Archaeological Science: Reports*, 12: 307–315. DOI: https://doi.org/10.1016/j.jasrep.2017.01.027

Pickering, TR, Heaton, JL, Clarke, RJ and **Stratford, D.** 2018. Hominin hand bone fossils from Sterkfontein Caves, South Africa (1998–2003 excavations). *Journal of Human Evolution*, 118: 89–102. DOI: https://doi.org/10.1016/j.jhevol.2018.02.014

Piperno, DR. 2006. *Phytoliths: A Comprehensive Guide for Archaeologists and Paleoecologists*. Oxford: Altamira Press.

Plug, I and **Mitchell, P.** 2008. Sehonghong: hunter-gatherer utilization of animal resources in the highlands of Lesotho. *Annals of the Transvaal Museum*, 45: 31–53.

Prescott, JR and **Hutton, JT.** 1994. Cosmic ray contributions to dose rates for luminescence and ESR dating: Large depths and long-term time variations. *Radiation Measurements*, 23: 497–500. DOI: https://doi.org/10.1016/1350-4487(94)90086-8

Riding, R. 2000. Microbial carbonates: the geological record of calcified bacterial-algal mats and biofilms. *Sedimentology*, 47(Suppl 1): 179–214. DOI: https://doi.org/10.1046/j.1365-3091.2000.00003.x

Riga, A, Mori, T, Pickering, TR, Moggi-Cecchi, J and **Menter, CG.** 2019. Ages-at-death distribution of the early Pleistocene hominin fossil assemblage from Drimolen (South Africa). *American Journal of Physical Anthropology*, 168: 632–636. DOI: https://doi.org/10.1002/ajpa.23771

Roberts, RG, Galbraith, RF, Yoshida, H, Laslett, GM and **Olley, JM.** 2000. Distinguishing dose populations in sediment mixtures: a test of single-grain optical dating procedures using mixtures of laboratory-dosed quartz. *Radiation Measurements*, 32: 459–465. DOI: https://doi.org/10.1016/S1350-4487(00)00104-9

Sampson, CG. 1968. *The Middle Stone Age industries of the Orange River scheme area*. Bloemfontein, South Africa: National Museum.

Sampson, CG. 1970. *The Smithfield industrial complex: further field results*. Bloemfontein, South Africa: National Museum.

Sampson, CG. 1972. *The stone age industries of the Orange River Scheme and South Africa*. Bloemfontein, South Africa: National Museum.

Sampson, CG, Moore, V, Bousman, CB, Stafford, B, Giordano, A and **Willis, M.** 2015. A GIS Analysis of the Zeekoe Valley Stone Age Archaeological Record in South Africa. *Journal of African Archaeology*, 13: 167–185. DOI: https://doi.org/10.3213/2191-5784-10277

Santisteban, JI, Mediavilla, R, López-Pamo, E, Dabrio, CJ, Blanca Ruiz Zapata, M, José Gil García, M, Castaño, S and **Martínez-Alfaro, PE.** 2004. Loss on ignition: a qualitative or quantitative method for organic matter and carbonate mineral content in sediments? *Journal of Paleolimnology*, 32: 287–299. DOI: https://doi.org/10.1023/B:JOPL.0000042999.30131.5b

Schoenenberger, PJ, Wysocki, DA, Benham, EC and **Broderson, WD.** 2002. *Field book for describing and sampling soils, version 2.0*. Lincoln, NE, USA: National Resource Conservation Service, National Soil Survey Center.

Scott, L, Neumann, FH, Brook, GA, Bousman, CB, Norström, E and **Metwally, AA.** 2012. Terrestrial fossil-pollen evidence of climate change during the last 26 thousand years in Southern Africa. *Quaternary Science Reviews*, 32: 100–118. DOI: https://doi.org/10.1016/j.quascirev.2011.11.010

Shaw, M, Ames, CJH, Phillips, N, Chambers, S, Dosseto, A, Douglass, M, Goble, R, Jacobs, Z, Jones, B, Lin, SCH, Low, M, McNeil, J-L, Nasoordeen, S, O'Driscoll, CA, Saktura, RB, Sumner, TA, Watson, S, Will, M and **Mackay, A.** 2019. The Doring River Archaeology Project: Approaching the evolution of human land use patterns in the Western Cape, South Africa. *PaleoAnthropology*, 2019: 400–422.

Sheldrick, BH and **Wang, C.** 1993. Particle Size Distribution. In: Carter, MR (ed.) *Soil sampling and methods of analysis*, 499–511. Boca Raton, USA: Lewis Publishers.

Smith, RMH. 1990. A review of stratigraphy and sedimentary environments of the Karoo Basin of South Africa. *Journal of African Earth Sciences (and the Middle East)*, 10: 117–137. DOI: https://doi.org/10.1016/0899-5362(90)90050-O

Stewart, BA, Dewar, GI, Morley, MW, Inglis, RH, Wheeler, M, Jacobs, Z and **Roberts, RG.** 2012. Afromontane foragers of the Late Pleistocene: Site formation, chronology and occupational pulsing at Melikane Rockshelter, Lesotho. *Quaternary International*, 270: 40–60. DOI: https://doi.org/10.1016/j.quaint.2011.11.028

Stewart, BA and **Mitchell, PJ.** 2018. Late Quaternary palaeoclimates and human-environment dynamics of the Maloti-Drakensberg region, southern Africa. *Quaternary Science Reviews*, 196: 1–20. DOI: https://doi.org/10.1016/j.quaint.2011.11.028

Truc, L, Chevalier, M, Favier, C, Cheddadi, R, Meadows, ME, Scott, L, Carr, AS, Smith, GF and **Chase, BM.** 2013. Quantification of climate change for the last 20,000 years from Wonderkrater, South Africa: Implications for the long-term dynamics of the Intertropical Convergence Zone. *Palaeogeography, Palaeoclimatology, Palaeoecology*, 386: 575–587. DOI: https://doi.org/10.1016/j.palaeo.2013.06.024

Wadley, L. 1995. Review of dated Stone Age sites recently excavated in the eastern Free State, South Africa. *South African Journal of Science*, 91: 574–579.

Wadley, L. 1996. The Robberg Industry of Rose Cottage Cave, Eastern Free State: The Technology, Spatial Patterns and Environment. *The South African Archaeological Bulletin*, 51: 64–74. DOI: https://doi.org/10.2307/3888841

Wadley, L. 1997. Rose Cottage Cave: archaeological work 1987 to 1997. *South African Journal of Science*, 93: 439–444.

Wadley, L. 2000a. The Early Holocene Layers of Rose Cottage Cave, Eastern Free State: Technology, Spatial Patterns and Environment. *The South African Archaeological Bulletin*, 55: 18–31. DOI: https://doi.org/10.2307/3888889

Wadley, L. 2000b. The Wilton and Pre-Ceramic Post-Classic Wilton Industries at Rose Cottage Cave and their Context in the South African Sequence. *The South African Archaeological Bulletin*, 55: 18–31. DOI: https://doi.org/10.2307/3888959

Wadley, L. 2004. Late Middle Stone Age spatial patterns in Rose Cottage Cave, South Africa. In: Conard, NJ (ed.), *Settlement dynamics of the Middle Paleolithic and Middle Stone Age II*, 23–36. Tübingen: Kerns Verlag.

Wintle, AG. 1997. Luminescence dating: laboratory procedures and protocols. *Radiation Measurements*, 27: 769–817. DOI: https://doi.org/10.1016/S1350-4487(97)00220-5

Zhao, Z and **Pearsall, DM.** 1998. Experiments for Improving Phytolith Extraction from Soils. *Journal of Archaeological Science*, 25: 587–598. DOI: https://doi.org/10.1006/jasc.1997.0262

How to cite this article: Ames, CJH, Gliganic, L, Cordova, CE, Boyd, K, Jones, BG, Maher, L and Collins, BR. 2020. Chronostratigraphy, Site Formation, and Palaeoenvironmental Context of Late Pleistocene and Holocene Occupations at Grassridge Rock Shelter (Eastern Cape, South Africa). *Open Quaternary*, 6: 5, pp. 1–19. DOI: https://doi.org/10.5334/oq.77

Submitted: 09 November 2019 **Accepted:** 19 February 2020 **Published:** 24 March 2020

]u[*Open Quaternary* is a peer-reviewed open access journal published by Ubiquity Press. OPEN ACCESS